Current Status of Post-Combustor Trace Chemistry Modeling and Simulation at NASA Glenn Research Center

Thomas Wey
Taitech, Inc., Beavercreek, Ohio

Nan-Suey Liu
Glenn Research Center, Cleveland, Ohio

March 2003

The NASA STI Program Office . . . in Profile

Since its founding, NASA has been dedicated to the advancement of aeronautics and space science. The NASA Scientific and Technical Information (STI) Program Office plays a key part in helping NASA maintain this important role.

The NASA STI Program Office is operated by Langley Research Center, the Lead Center for NASA's scientific and technical information. The NASA STI Program Office provides access to the NASA STI Database, the largest collection of aeronautical and space science STI in the world. The Program Office is also NASA's institutional mechanism for disseminating the results of its research and development activities. These results are published by NASA in the NASA STI Report Series, which includes the following report types:

- TECHNICAL PUBLICATION. Reports of completed research or a major significant phase of research that present the results of NASA programs and include extensive data or theoretical analysis. Includes compilations of significant scientific and technical data and information deemed to be of continuing reference value. NASA's counterpart of peer-reviewed formal professional papers but has less stringent limitations on manuscript length and extent of graphic presentations.

- TECHNICAL MEMORANDUM. Scientific and technical findings that are preliminary or of specialized interest, e.g., quick release reports, working papers, and bibliographies that contain minimal annotation. Does not contain extensive analysis.

- CONTRACTOR REPORT. Scientific and technical findings by NASA-sponsored contractors and grantees.

- CONFERENCE PUBLICATION. Collected papers from scientific and technical conferences, symposia, seminars, or other meetings sponsored or cosponsored by NASA.

- SPECIAL PUBLICATION. Scientific, technical, or historical information from NASA programs, projects, and missions, often concerned with subjects having substantial public interest.

- TECHNICAL TRANSLATION. English-language translations of foreign scientific and technical material pertinent to NASA's mission.

Specialized services that complement the STI Program Office's diverse offerings include creating custom thesauri, building customized databases, organizing and publishing research results . . . even providing videos.

For more information about the NASA STI Program Office, see the following:

- Access the NASA STI Program Home Page at *http://www.sti.nasa.gov*

- E-mail your question via the Internet to help@sti.nasa.gov

- Fax your question to the NASA Access Help Desk at 301–621–0134

- Telephone the NASA Access Help Desk at 301–621–0390

- Write to:
  NASA Access Help Desk
  NASA Center for AeroSpace Information
  7121 Standard Drive
  Hanover, MD 21076

NASA/TM—2003-212184

Current Status of Post-Combustor Trace Chemistry Modeling and Simulation at NASA Glenn Research Center

Thomas Wey
Taitech, Inc., Beavercreek, Ohio

Nan-Suey Liu
Glenn Research Center, Cleveland, Ohio

National Aeronautics and
Space Administration

Glenn Research Center

March 2003

Acknowledgments

1 Introduction

The overall objective of the current effort at NASA GRC is to evaluate, develop and apply methodologies suitable for modeling intra-engine trace chemical changes over post combustor flow path relevant to the pollutant emissions from aircraft engines [1, 2]. At the present time, the focus is the high pressure turbine environment. At first, the trace chemistry model of CNEWT [1, 2] were implemented into GLENN-HT [3] as well as NCC [4]. Then, CNEWT, CGLENN-HT and NCC were applied to the trace species evolution in a cascade of Cambridge University's No.2 rotor and in a turbine vane passage. In general, the results from these different codes provide similar features. However, the details of some of the quantities of interest can be sensitive to the differences of these codes. This report summaries the implementation effort and presents the comparision of the NO.2 rotor results obtained from these different codes. The comparison of the turbine vane passage results is reported in [5].

In addition to the implementation of trace chemistry model into existing CFD codes, several pre/post-processing tools that can handle the manipulations of the geometry, the unstructured and structured grids as well as the CFD solutions also have been enhanced and seamlessly tied with NCC, CGLENN-HT and CNEWT. Thus, a complete CFD package consisting of pre/post-processing tools and flow solvers suitable for post-combustor intra-engine trace chemistry study is assembled.

2 Codes Acquired from MIT

The programs acquired initially from MIT were

- CNEWT — A compressible Navier-Stokes flow solver which utilizes a single rotating frame of reference for rotating turbine blades, the unstructured tetrahedral grids for finite-volume discretization, a $k - \epsilon$ model for the turbulence closure, and a passive finite-rate reactive flow[1] for trace chemistry. A simple MPI (Message Passing Interface) procedure was implemented at the subroutine level to compute the species production rate.

- CALCHEM — 1-D version of CNEWT.

- CKINTERP — CHEMKIN II interpreter for reaction rate parameters and chemical mechanism.

- cfe_NASA — A MATLIB script to generate species inlet conditions using CHEMKIN III libraray which is a commercial extension of CHEMKIN II. The trace chemistry mechanism currently has twenty five species and seventy four reaction steps.

---

[1]The passive finite-rate reacting flow means that the transport coefficients of the mixture, such as molecular viscosity, molecular thermal conductivity are independent of mass fraction of species, so are the specific heat at constant pressure and the ratio of the specific heats.

3   Pre-Processing

The main pre-processing tools are computer programs called FPLOT and T3D. Briefly, FPLOT is an ensemble of utility routines for generating the structured and unstructured meshes as well as viewing the solutions of CFD. Furthermore, it has the ability to digitize IGES files from other CAD packages. It will digitize the IGES untrimmed entities into representable data in PLOT3D format, and trimmed entities as unstructured quadrilateral elements. It also has the ability to build surface quadrilateral meshes out of the geometry almost automatically. Additionally, the ability to generate overset [6] or conforming [7] unstructured hexahedral meshes has been added for advanced users. The graphical user interface (GUI) of FPLOT is based upon FLTK (pronounced "fulltick", which is an open-sourced C++ user interface toolkit for X Window, MS Windows XP/2000/NT/98/95 and Mac OS X), which can be downloaded from *www.fltk.org*. T3D is a predecessor of FPLOT, and it is based upon SGI graphics library (GL) and XFORMS[2] user interface. In short, it is a structured as well as an unstructured mesh generation program. It can also be used as a post-processing program for CFD solutions.

A summary of the current effort in this area follows:

- Geometry acquiring tools

    1. Import of CAD data — FPLOT can read geometry files in the following formats:

        (a) IGES format
        (b) PATRAN neutral format
        (c) STL (stereolithography) format
        (d) FPLOT format
        (e) Plot3d format
        (f) FAST format
        (g) Lockheed ACAD format

        The preferred format of the data is IGES.

    2. Creation of commonly used geometry shapes — T3D is used here to build and create simple geometries. The effort of porting the entire functionalities of T3D to FPLOT is continuing under the current project.

- Grid generation tools

    1. Conforming grids — The default meshes used by CNEWT, GLENN-HT and NCC are conforming grids. The point-to-point constraints make the generation of very high quality viscous grids for complicated geometries a time consumming job. Both T3D and FPLOT are used to generate the grids for the current project. A module for generating the unstructured all-hexahedral mesh has been added to FPLOT. The underlined algorithm of this module

---

[2]XFORMS is a graphical user interface toolkit for X Window Systems and can be freely downloaded from *ftp://ncmir.ucsd.edu/pub/xforms/OpenSource*

was described in [7]. The effort of implmenting another algorithm for generating hexahedral-dominant unstructured mesh is in pending. Other commercial grid generators may be used as well to generate conforming structurd grid for CGLENN-HT or unstructured grid for NCC.

2. Non-conforming grids — Overset grid techniques allow each component or partition of a given configuration to be gridded independently and then superimposed to form a composite of overset meshes for CFD simulations. The point-to-point constraints are relaxed so that it makes the generation of very high quality viscous grids for complicated geometries a less time consuming job. The overset grid option has been implemented into CNEWT, CGLENN-HT and NCC for any rapid prototyping CFD application. In the present work, T3D is used to generate the component grids and OVERGC[8], acronym of overset grid communicator, is used to build the grid interfaces among the component grids. FPLOT[6] is then utilized to convert the composite grids to overset unstructured grids for CNEWT and NCC, or overset structured grids for CGLENN-HT. FPLOT is also used to tag the boundary elements and fluid elements for the NCC and CNEWT. This capability of generalized grid interface allows the geometry and mesh generation of complex systems to be dealt with via a 'divide and conquer' approach. The analyst can assemble the definition for a complex system by pulling together meshes from independently created components, thereby greatly reducing the amount of time spent on the overall mesh generation.

- Graphics user interface (GUI) for GLENN-HT — To reduce the tedious and time consuming preparation process, a module is implemented into FPLOT to allow users to graphically prepare the block connectivity of the conforming grids, the boundary conditions and the initial conditions for GLENN-HT. (see in Figure 1.)
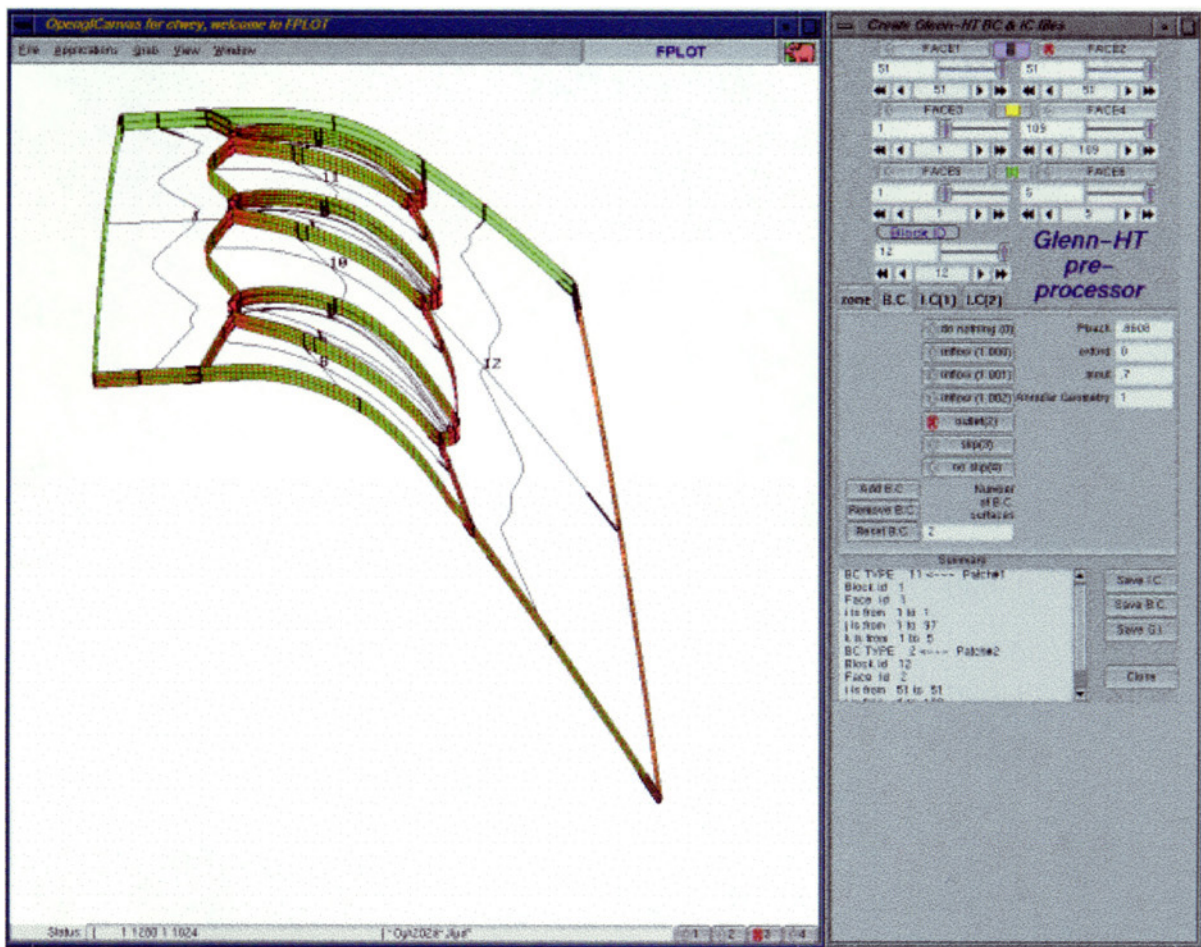
Figure 1: Using FPLOT to prepare boundary and initial conditions for GLENN-HT.

4 CNEWT/GRC

The original CNEWT developed at MIT (CNEWT/MIT) has been enhanced under the current effort, this enhanced version is termed as CNEWT/GRC[3]. A description of the enhancements follows:

- Dynamic allocation of memory – C routines are used here to achieve the goal. It results in mixed FORTRAN and C source codes.

- Type of elements — In addition to tetrahedral element, hexahedral, wedge and pyramid elements are added to CNEWT/GRC.

- Overset/chimera grid capability has been added for rapid prototyping.

- Multiple rotating frames of reference (MRF) for rotating grids— For a single rotating reference frame, the entire mesh in a computational model can rotate at constant angular velocity ($\vec{\omega}$) about a prescribed axis. The same feature is extended to multiple rotating frames of reference, in which different angular velocities (and even different rotating axes) are assigned to different mesh blocks or groups within the model. Balance equations for each group are expressd in the relative reference frame but in terms of the absolute velocity (i.e. the velocity with respect to a stationary coordinate system), and this leads to a hybrid formulation of the balance equations.

Continuity equation:

$$\frac{d}{dt}\iiint_V \rho\, dV + \iint_A \rho(\vec{u} - \vec{U_g}) \cdot d\vec{A} = 0$$

Species transport equation:

$$\frac{d}{dt}\iiint_V \rho_m\, dV + \iint_A \rho_m(\vec{u} - \vec{U_g}) \cdot d\vec{A} = \iint_A \rho D_{eff}\nabla(\frac{\rho_m}{\rho}) \cdot d\vec{A} + \dot{w}_m$$

Momentum equation:

$$\frac{d}{dt}\iiint_V \rho\vec{u}\, dV + \iint_A \rho\vec{u}(\vec{u} - \vec{U_g}) \cdot d\vec{A} = -\iint_A pd\vec{A} + \iint_A \tau \cdot d\vec{A}$$
$$- \iiint_V \rho\vec{\omega_g} \times \vec{u}\, dV$$

Energy equation:

$$\frac{d}{dt}\iiint_V \rho E\, dV + \iint_A \rho E(\vec{u} - \vec{U_g}) \cdot d\vec{A} = -\iint_A p\vec{u} \cdot d\vec{A} - \iint_A \vec{q} \cdot d\vec{A}$$
$$+ \iint_A \vec{u} \cdot \tau \cdot d\vec{A}$$

---

[3]An alternative name for the CNEWT/GRC is TEXANS, acronym of **TE**trahedal and he**XA**hedral **N**avier-**S**tokes solver.

Turbulence equations:

$$\frac{d}{dt}\iiint_V \rho k \, dV + \iint_A \rho k(\vec{u} - \vec{U_g}) \cdot d\vec{A} = S_k + \iint_A (\mu + \frac{\mu_T}{\sigma_k})\nabla k \cdot d\vec{A}$$

$$\frac{d}{dt}\iiint_V \rho \epsilon \, dV + \iint_A \rho \epsilon (\vec{u} - \vec{U_g}) \cdot d\vec{A} = S_\epsilon + \iint_A (\mu + \frac{\mu_\epsilon}{\sigma_\epsilon})\nabla \epsilon \cdot d\vec{A}$$

where

$$\vec{q} = -\kappa \nabla T$$

$$\tau = -\frac{2}{3}\mu(\nabla \cdot \vec{u})\mathbf{I} + \frac{1}{2}\mu(\nabla \vec{\mathbf{u}} + (\nabla \vec{\mathbf{u}})^{\mathbf{T}})$$

where V is an arbitrary control volume with control surface A, ρ is the fluid density, ρ_m is the partial density of species m, $\dot{w}_m$ is the production rate of species m, $\vec{u}$ is the flow velocity in a stationary Cartesian coordinate system, $\vec{\omega_g}$ is the grid rotating velocity for each designated axis, $\vec{U_g} = \vec{\omega_g} \times \vec{r}$, E is the total energy density, k is the turbulent kinetic energy, ϵ is the turbulent dissipation rate, S_k is the source term for k, S_ϵ is the source term for ϵ, p is the static pressure, τ is the viscous stress tensor, $\vec{q}$ is the heat flux vector, D_{eff} is the effective mass diffusivity coefficient which is equal to $\frac{\mu_{eff}}{\rho Sc}$, κ and μ are the thermal conductivity and viscosity coefficients, respectively. For gas, the Schmidt number (Sc) is about 1.

This formulation is userful for the following applications:

1. flow in turbomachinery

2. flow in torque converters

3. flow in mixing vessels

4. flow in axial and centrifugal pumps

5. flow in ducted fans

- Sliding mesh – The sliding mesh technique is ideally suited for problems involving rotor/stator interactions. It is presumbly the most accurate and straightforward method for a turbomachinery calculation. It starts by dividing the computational mesh into stationary groups/blocks and rotating groups/blocks. They are connected to each other through a slightly overlapped sliding surface. The governing equations must be time dependent. The information transfer across the interface is accomplished by using the conventional overset grid interpolation. This option in CNEWT/GRC is yet to be fully validated.

- Arbitrary Lagrangian-Eulerian formulation

  In order to handle the moving frames of reference associated with the moving mesh, the partial differential equtions need to be modified. This is most easily accomplished by the Arbitrary Largrangian-Eulerian (ALE) formulation. The integrated

mass, momentum, and energy equations over a moving control volume for the gas phase may be written as:

Continuity equation:

$$\frac{d}{dt}\iiint_{V(t)}\rho\,dV + \iint_{A(t)}\rho(\vec{u}-\vec{U}_g)\cdot d\vec{A} = -\iiint_{V(t)}\rho\nabla\cdot\vec{U}_g\,dV$$

Species transport equation:

$$\frac{d}{dt}\iiint_{V(t)}\rho_m\,dV + \iint_{A(t)}\rho_m(\vec{u}-\vec{U}_g)\cdot d\vec{A} = \iint_{A(t)}\rho D_{eff}\nabla(\frac{\rho_m}{\rho})\cdot d\vec{A} + \dot{w}_m$$
$$- \iiint_{V(t)}\rho_m\nabla\cdot\vec{U}_g\,dV$$

Momentum equation:

$$\frac{d}{dt}\iiint_{V(t)}\rho\vec{u}\,dV + \iint_{A(t)}\rho\vec{u}(\vec{u}-\vec{U}_g)\cdot d\vec{A} = -\iint_{A(t)}p\,d\vec{A} + \iint_{A(t)}\tau\cdot d\vec{A}$$
$$- \iiint_{V(t)}\rho\vec{u}\nabla\cdot\vec{U}_g\,dV$$

Energy equation:

$$\frac{d}{dt}\iiint_{V(t)}\rho E\,dV + \iint_{A(t)}\rho E(\vec{u}-\vec{U}_g)\cdot d\vec{A} = -\iint_{A(t)}p\vec{u}\cdot d\vec{A} - \iint_{A(t)}\vec{q}\cdot d\vec{A}$$
$$+ \iint_{A(t)}\vec{u}\cdot\tau\cdot d\vec{A}$$
$$- \iiint_{V(t)}\rho E\nabla\cdot\vec{U}_g\,dV$$

Turbulence equations:

$$\frac{d}{dt}\iiint_{V(t)}\rho k\,dV + \iint_{A(t)}\rho k(\vec{u}-\vec{U}_g)\cdot d\vec{A} = S_k + \iint_{A}(\mu+\frac{\mu_T}{\sigma_k})\nabla k\cdot d\vec{A}$$
$$- \iiint_{V(t)}\rho k\nabla\cdot\vec{U}_g\,dV$$

$$\frac{d}{dt}\iiint_{V(t)}\rho\epsilon\,dV + \iint_{A(t)}\rho\epsilon(\vec{u}-\vec{U}_g)\cdot d\vec{A} = S_\epsilon + \iint_{A}(\mu+\frac{\mu_\epsilon}{\sigma_\epsilon})\nabla\epsilon\cdot d\vec{A}$$
$$- \iiint_{V(t)}\rho\epsilon\nabla\cdot\vec{U}_g\,dV$$

where

$$\vec{q} = -\kappa\nabla T$$

$$\tau = -\frac{2}{3}\mu(\nabla\cdot\vec{u})\mathbf{I} + \frac{1}{2}\mu(\nabla\vec{u}+(\nabla\vec{u})^{\mathbf{T}})$$

where $V(t)$ is an arbitrary control volume with control surface $A(t)$, both are functions of time. Also, ρ is the fluid density, ρ_m is the partial density of species m, $\dot{w}_m$ is the production rate of species m, $\vec{u}$ is the flow velocity in a stationary Cartesian coordinate system, $\vec{U}_g$ is the grid velocity, E is the total energy density, k is the turbulent kinetic energy, ϵ is the turbulent dissipation rate, S_k is the source term for k, S_ϵ is the source term for ϵ, p is the static pressure, τ is the viscous stress tensor, $\vec{q}$ is the heat flux vector, D_{eff} is the effective mass diffusivity coefficient which is equal to $\frac{\mu_{eff}}{\rho Sc}$, κ and μ are the thermal conductivity and viscosity coefficients, respectively. For gas, Sc is about 1.

For a domain in the sliding mesh mode, the ALE form of the governing equations is simplified by the assumption that the mesh associated with the rotor is in rigid body rotation. The term $\nabla \cdot \vec{U}_g$ on the right hand side of the equations vanishes and $\vec{U}_g$ is just $\vec{\Omega} \times \vec{r}$, where $\vec{r}$ is the radius from the rotating axis, $\vec{\Omega}$ is the rotating velocity of the rigid body.

5   CGLENN-HT

GLENN-HT of version 3.1 (March 1999) was acquired from the Turbine Branch, NASA GRC. It is a Navier-Stokes compressible flow solver for the calorically perfect gas. It uses a single rotating frame of reference for rotating turbine blades, the multi-block structured grids for finite-volume discretization, a $k - \omega$ model for the turbulence closure, and a multigrid algorithm for convergence acceleration. Neither OpenMP (Multi Processing) nor MPI is implemented in the version 3.1.

This version was enhanceed into CGLENN-HT. A description of the enhancements follows:

- Dynamic allocation of memory – C routines are used here to achieve the goal. It results in mixed FORTRAN and C source codes.

- Overset/chimera grid capability — A major advantage of the overset approach is that the individual grid blocks can be superimposed to form a composite of meshes for CFD computations without subject to the usual point conforming restrictions due to the multi-block structured grids. It retains the computational efficiency associated with the use of the structured grids.

- Implementation of species transport equations —

$$\frac{d}{dt}\iiint_V \rho_m \, dV + \iint_A \rho_m (\vec{u} - \vec{U}_g) \cdot d\vec{A} = \iint_A \rho D_{eff} \nabla (\frac{\rho_m}{\rho}) \cdot d\vec{A} + \dot{w}_m$$

- Using Chemkin-II v.4.3 library and variable coefficient ordinary differential equation solver (VODE) for species production rate — A simple MPI procedure is implemented to compute the species production rate. Since the parallelism is implemented at the local subroutine level, other parts of the computation is still running in serial mode.

- Roe flux differencing — For convective flux terms, Roe's characteristic-based flux-difference splitting scheme is implemented as an alternative to the central difference with artificial dissipation.

- Alternative species gradient calculations — This method uses non-overlapping control volumes and stores the species gradient at the cell center of the grid for mass diffusion integration.

6   NCC

NCC v.1.0.8 is a general purpose Navier-Stokes compressible and incompressible flow solver based upon conforming unstructured grids. It can handle gaseous species and liquid fuels. The turbulence are modeled by the $k - \epsilon$ equations. PVM and MPI are implemented in the current version for massively parallel computing platforms.

A description of the enhancements follows:

- Enhancements to NCC pre-processor — GEN_FILES is modified so that it can convert a grid interface file created by FPLOT to *ncc_overset.bin* as an optional input file for NCC.

- Enhancements to NCC post-processor — NODAL_RESULTS is modified to be able to write data files in FPLOT and FIELDVIEW formats for either rotational or stationary coordinate system.

- Enhancements to NCC solver

  1. overset/chimera grid capability — Unstructured overset/chimera grid makes the mesh generation even easier than the regular unstructured grid.

  2. Multiple rotational reference frame (MRF) for rotational grids — It enables quasi-steady stator/rotor interaction simulations. It facilitates the analysis of the flow throughout the whole turbine by taking into account of the stator-rotor interaction while avoiding the potentially inaccurate boundary conditions imposed among the components. However, when compared to separate simulations for each component, such coupled calculations require larger domain and longer computing time. Separate analysis for each component is much faster, but it is essential to know when coupled analysis must be performed and what are the differences between separate and coupled analyses. It is well known that the separate analysis usually overpredicts flow energy losses in all turbine parts and only coupled analysis is suitable for accurate prediction of turbine efficiency.

  3. Multiple dissipation zones — Following the spirit of the multiple rotational reference frame, the dissipation coefficients and CFL number can be set to different values for each zone to achieve better convergency.

  4. Initial conditions — In stead of the 80 columns limitation, it uses a data file to input initial species conditions.

5. Total pressure and total temperature inlet boundary conditions — Total pressure and total temperature are specified at the inlet. This is more in line with other turbomachinery CFD codes. Both radial and circumferencial non-uniform profiles of the inlet conditions are implemented.

6. Total temperature and mass flux inlet boundary conditions are implemented.

7. Isothermal wall boundary condition — CNEWT style isothermal wall boundary condition is implemented.

8. Using Chemkin-II v.4.3 library and variable coefficient ordinary differential equation solver (VODE) for species production rate - this is an addition to the original NCC chemistry solver.

9. Roe flux differencing — For convective flux terms, Roe's characteristic-based flux-difference splitting scheme is implemented as an alternative to the central difference with artificial dissipation.

10. Alternative form of energy equation — For steady-state computation, the default dependent variable for the energy equation is the static enthalpy. In the alternative form, the total energy is the dependent variable to be solved.

11. Passive trace chemistry model — In this model, the transport coefficients of the mixture, such as molecular viscosity, molecular thermal conductivity are independent of the mass fractions of species, so are the specific heat at constant pressure and the ratio of the specific heats. It is the same model as that in CNEWT. It is noted here that, in the CGLENN-HT code, the molecular viscosity of the mixture is calculated using a power-law for its dependence on temperature.

7 Post-Processing

A description of the enhancements follows:

- Data reduction of the structured and unstructured grid flow solutions — To rapidly conduct sensitivity, parametric and trend analyses along a typical post-combustor intra-engine flow path, a module, which can dynamically apply data reduction technique to a set of three-dimensional CFD solutions to yield one dimensional data has been implemented into FPLOT. Three options are available for computing the averaged variables along the dominant flow path in the domain, they are area-weighted average, mass flux-weighted average and density-weighted average.

- Visualization of structured and unstructured grid flow solutions — In addition to data reduction, FPLOT is also used to visualize and interrogate the vast three-dimensional CFD results.

8   Examples

8.1   A Generic Stator-Rotor Configuration in MRF

To test the options of multiple reference frames (MRF) and overset grid, a generic stator-rotor configuration is created and gridded using T3D and OVERGC. Then FPLOT is used to tag the identification of the boundary patches and fluid elements so that the different rotaional speeds can be assigned to the stator and the rotor with ease. A typical turbine case is selected for NCC and CNEWT/GRC: the total pressure at the inlet is 1629080 N/M^2, the total temperature is 1645 K at the inlet, the exit pressure is 985627 N/M^2, the blade wall temperature is 956 K, and the rotating speed of the rotor is 8868 RPM. In addition, a chemically frozen flow is assumed. The pressure distribution and the relative velocity vector of the NCC solution are shown in Figure 2 and Figure 3. The pressure distribution and the relative velocity vector of the CNEWT/GRC solution are shown in Figure 4 and Figure 5.
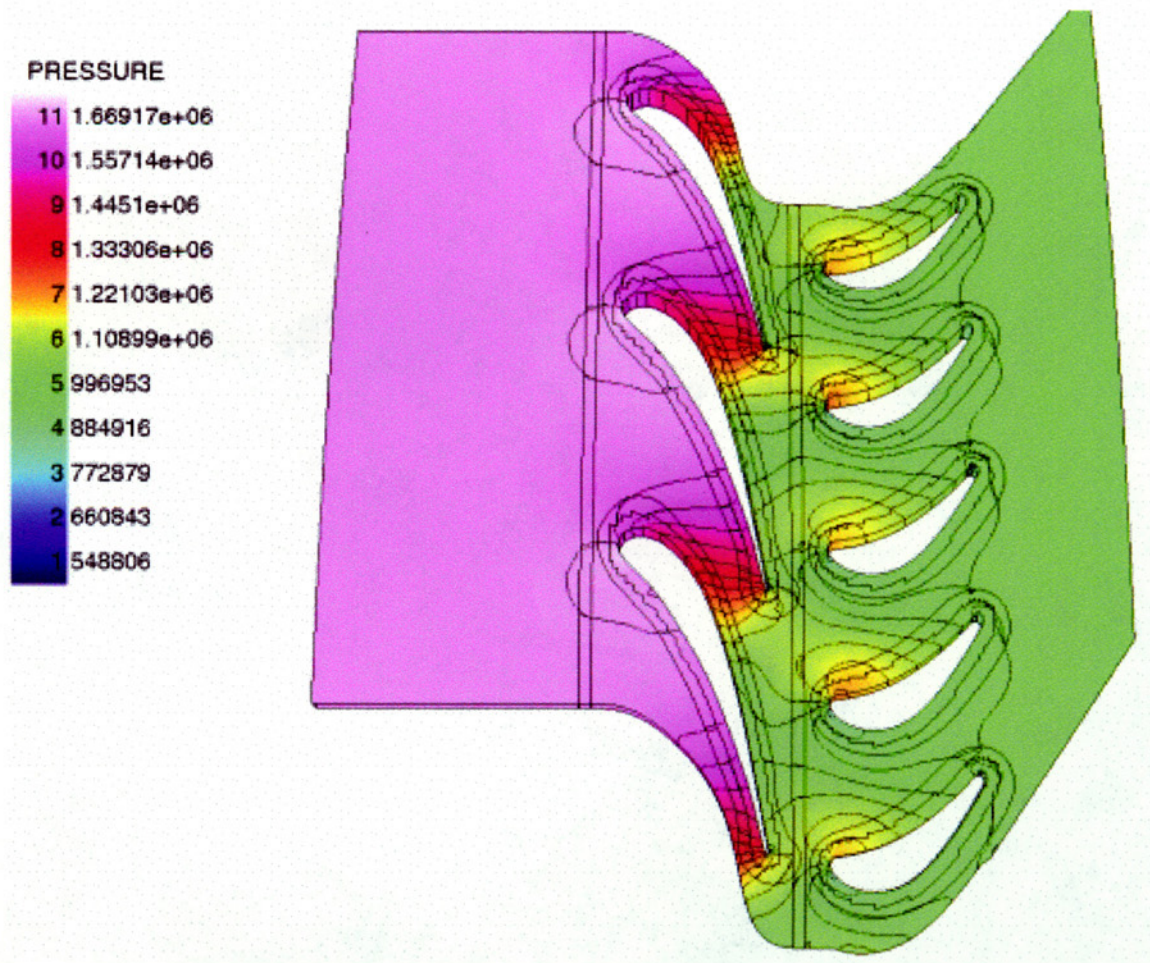
Figure 2: A stage of the generic stator-rotor rows using NCC — quasi-steady pressure contours.
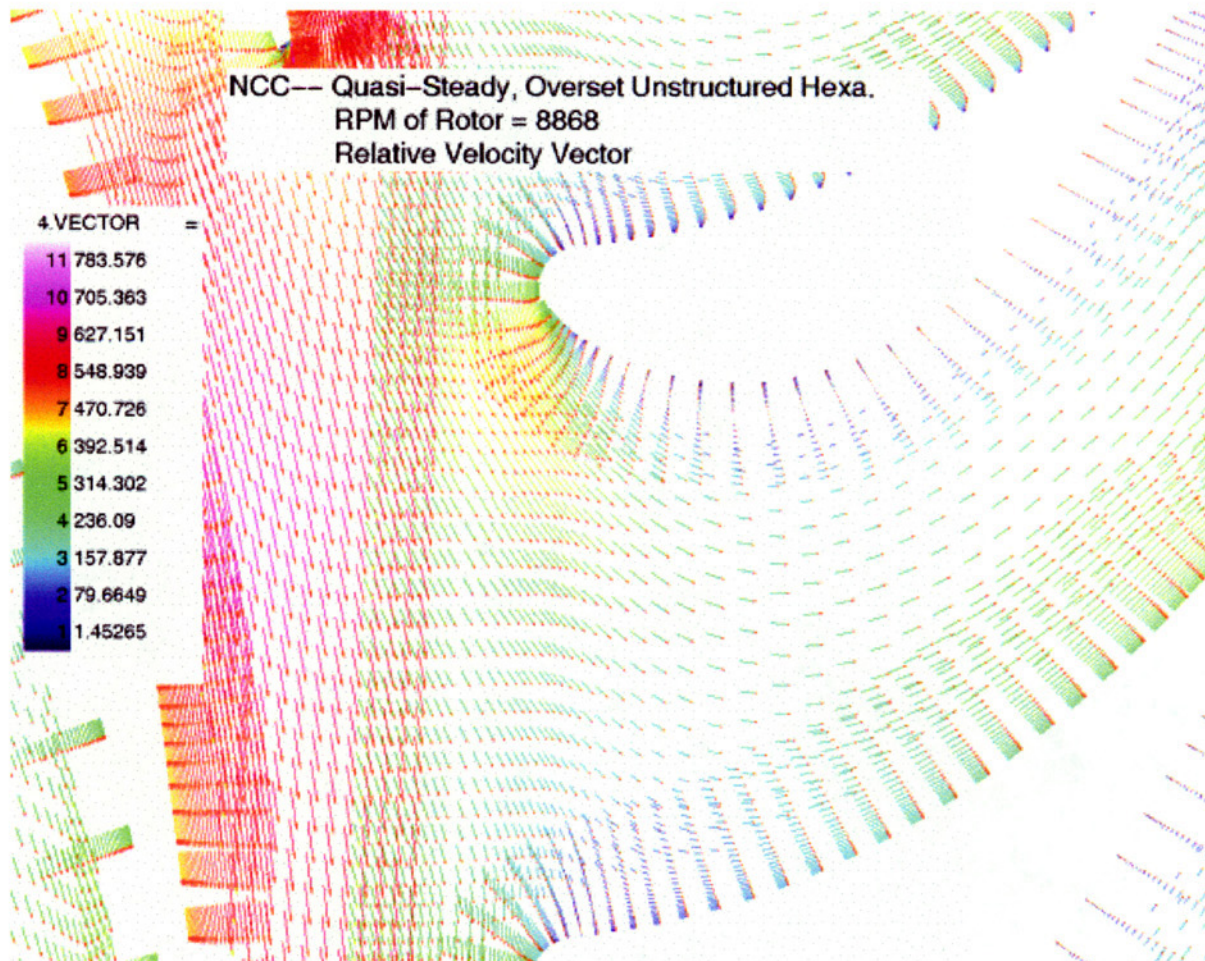
Figure 3: A stage of the generic stator-rotor rows using NCC — quasi-steady relative velocity vectors.
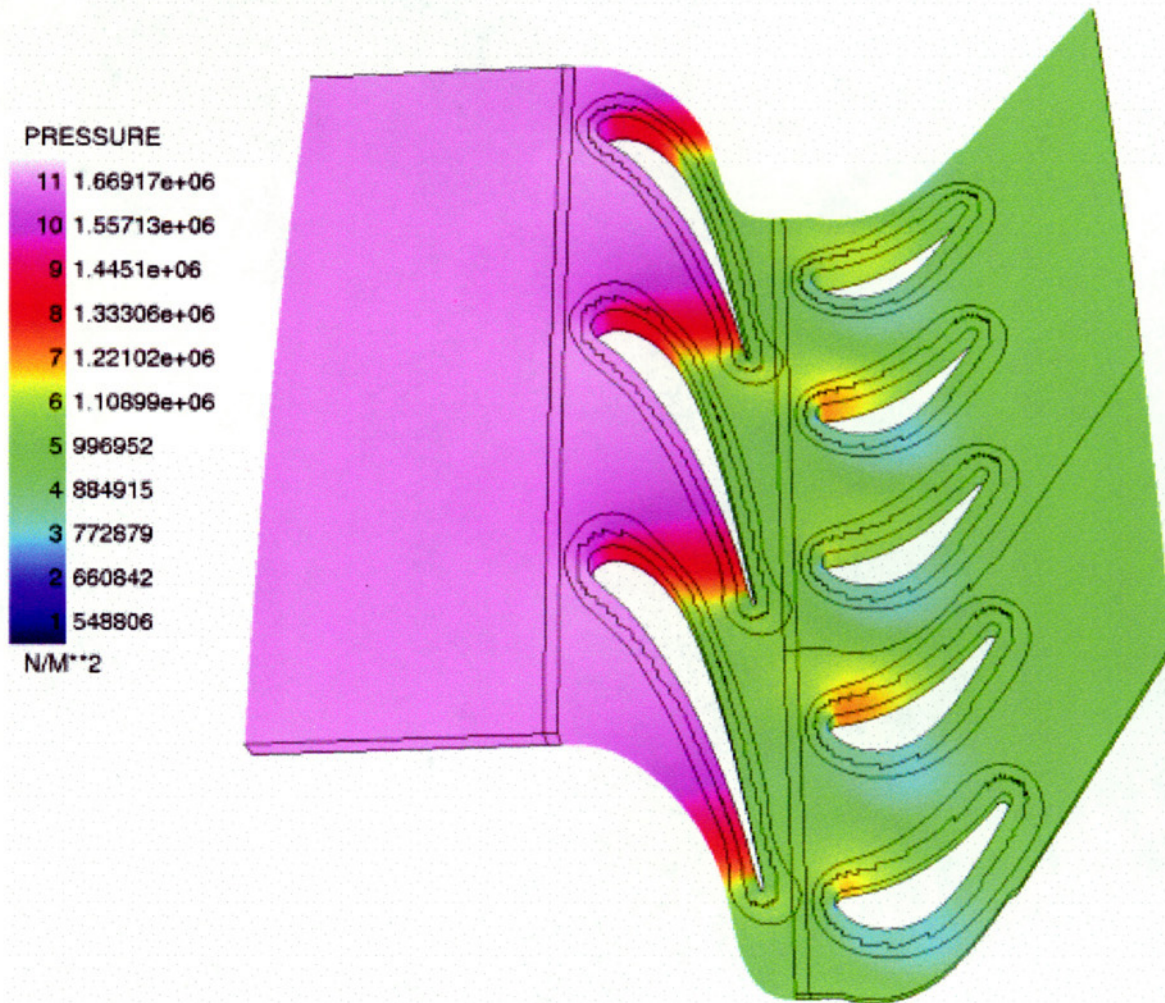
Figure 4: A stage of the generic stator-rotor rows using CNEWT/GRC — quasi-steady pressure contours.
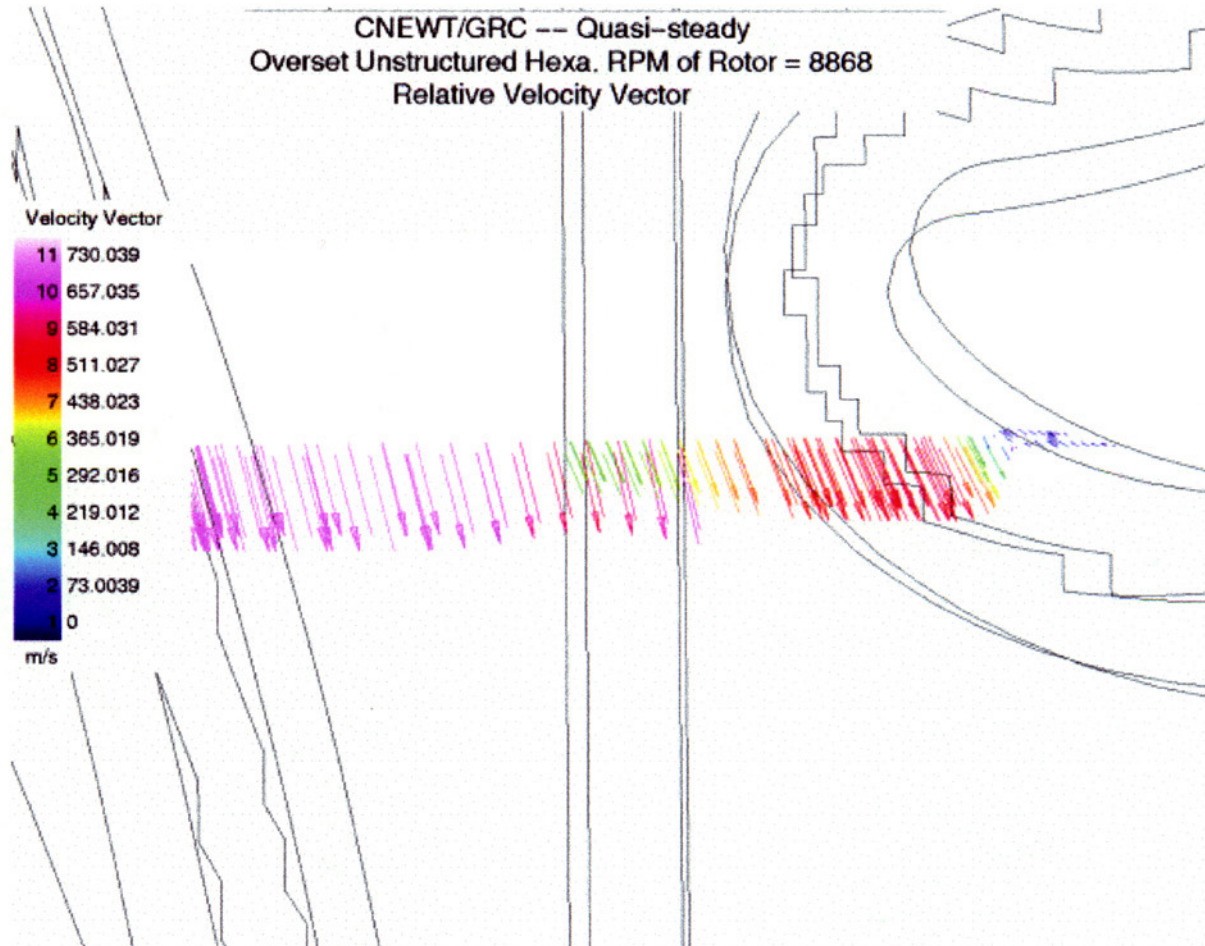
Figure 5: A stage of the generic stator-rotor rows using CNEWT/GRC — quasi-steady relative velocity vectors. Most of the velocity vectors are omitted so that the velocity transition from the stationary reference frame of the stator to the relative reference frame of the rotor can be viewed clearly.

8.2 A Generic Stator-Rotor Interaction Using the Sliding Mesh Option

To test the sliding mesh capability implemented into CNEWT/GRC *(also known as TEXANS)*, the previous example is computed in the sliding mesh mode. The pressure, temperature and Mach number distributions are shown in Figure 6, Figure 7 and Figure 8 respectively.
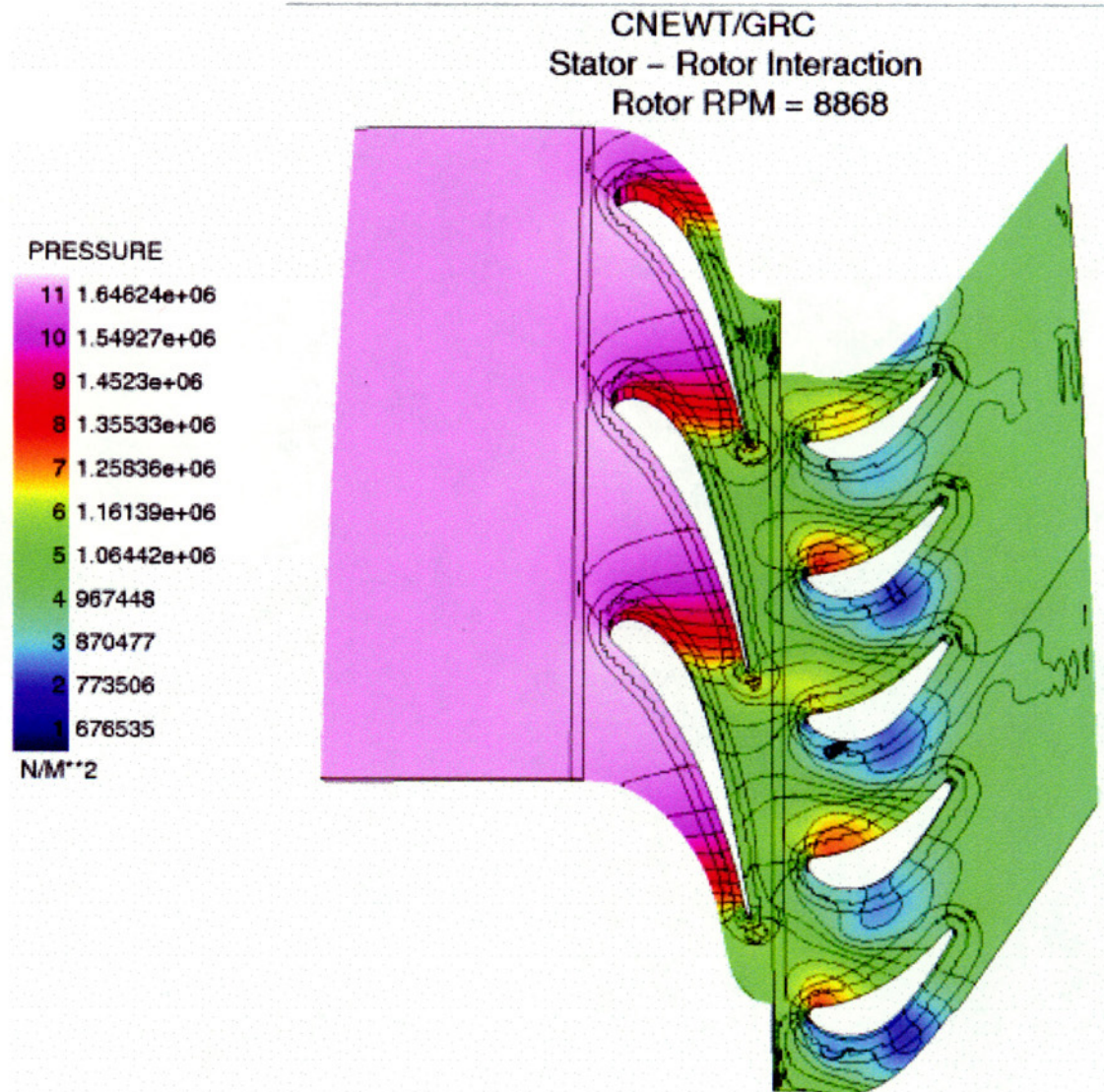
Figure 6: A stage of the generic stator-rotor rows using CNEWT/GRC *(also known as TEXANS)* — unsteady pressure contours.
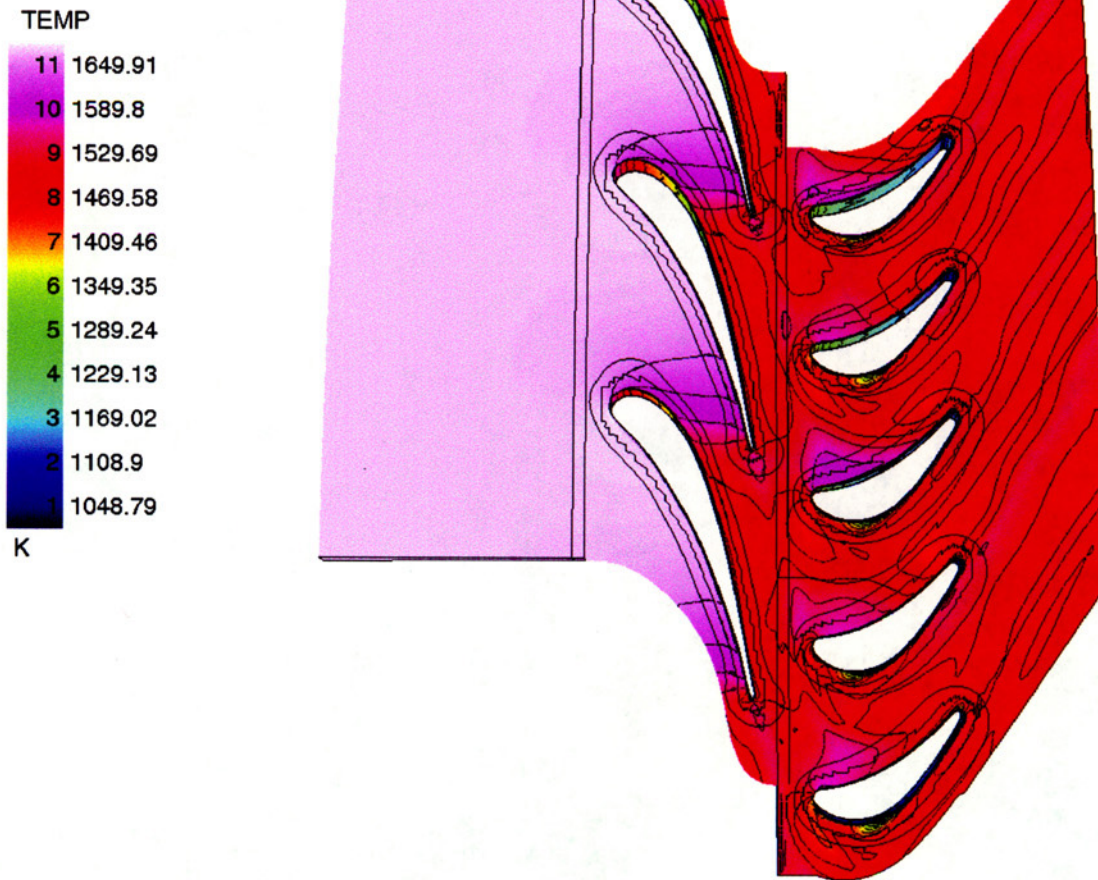
Figure 7: A stage of the generic stator-rotor rows using CNEWT/GRC *(also known as TEXANS)* — unsteady temperature contours.
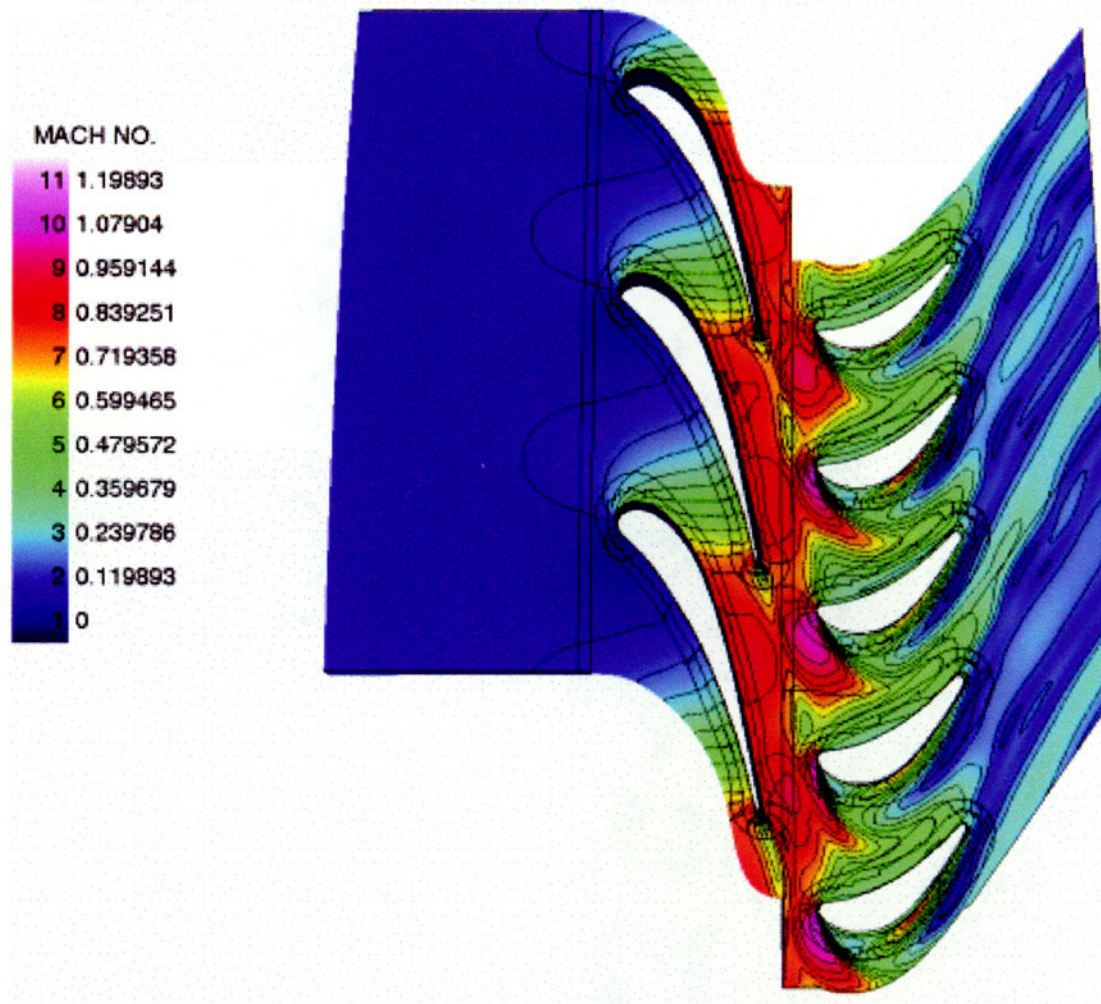
Figure 8: A stage of the generic stator-rotor rows using CNEWT/GRC *(also known as TEXANS)* — unsteady Mach number contours.

8.3 Cambridge No. 2 Rotor

Homogeneous inlet conditions are used and the blade row is simulated in the rotor relative frame using three blade passages. The angular velocity is 2600 rpm at a radius of about .065 meter. At the inlet, the total pressure of the mainstream hot gas is set to be 907351 N/M^2; the specific heat at constant pressure is 1184 $J/kg\ K$; the ratio of specific heats is 1.32. Following standard practice, the value of the turbulence intensity is assumed to be 2.5% of the computed inlet normal velocity, while the turbulence length scale at the inlet is set to be .05 m. At the exit, the static pressure is set to be 781057.9 N/M^2, i.e. 86.1% of the inlet total pressure. The surface temperature of the blade is 1000 K.

Since transport properties are evaluated differently in different codes, they are summarized as the following three options:

a. Option 1 — The temperature is iteratively computed from the static enthalpy of the gas mixture, h, and the specific heat at constant pressure of the gas mixture, C_p. In addition, the gas constant of the mixture, the specific heat at constant pressure of the gas mixture, laminar viscosity of the mixture and thermal conductivity of the mixture are all functions of species mass fractions and the temperature.

b. Option 2 — The temperature is computed from the enthalpy of the gas mixture, h and a constant C_p. Gas constant of the mixture, specific heat at constant pressure of the gas mixture, C_p, laminar viscosity of the mixture and thermal conductivity of the mixture are all constants which are either user specified parameters or computed via other parameters such as the Prandtl number.

c. Option 3 — The gas constant of the mixture and the specific heat at constant pressure of the gas mixture, C_p, are constants provided by the users. The laminar viscosity of the mixture is calculated using a power-law for its dependence on temperature.. The thermal conductivity of the mixture is computed through Prandtl number and C_p. The temperature is computed from the equation of state.

8.3.1 Relative Inlet Boundary Condition

The relative total temperature is 1631.7 K and the relative swirl angle is 26°, viewed from a rotating reference frame. The solutions of NCC and CGLENN-HT were presented from Figure 9 to Figure 15. The difference of solution between NCC's option 1 and 2 is negligible in this case from the point of view of trace chemistry. However, NO and SO_2 display larger differences between the solution from NCC and that from CGLENN-HT.
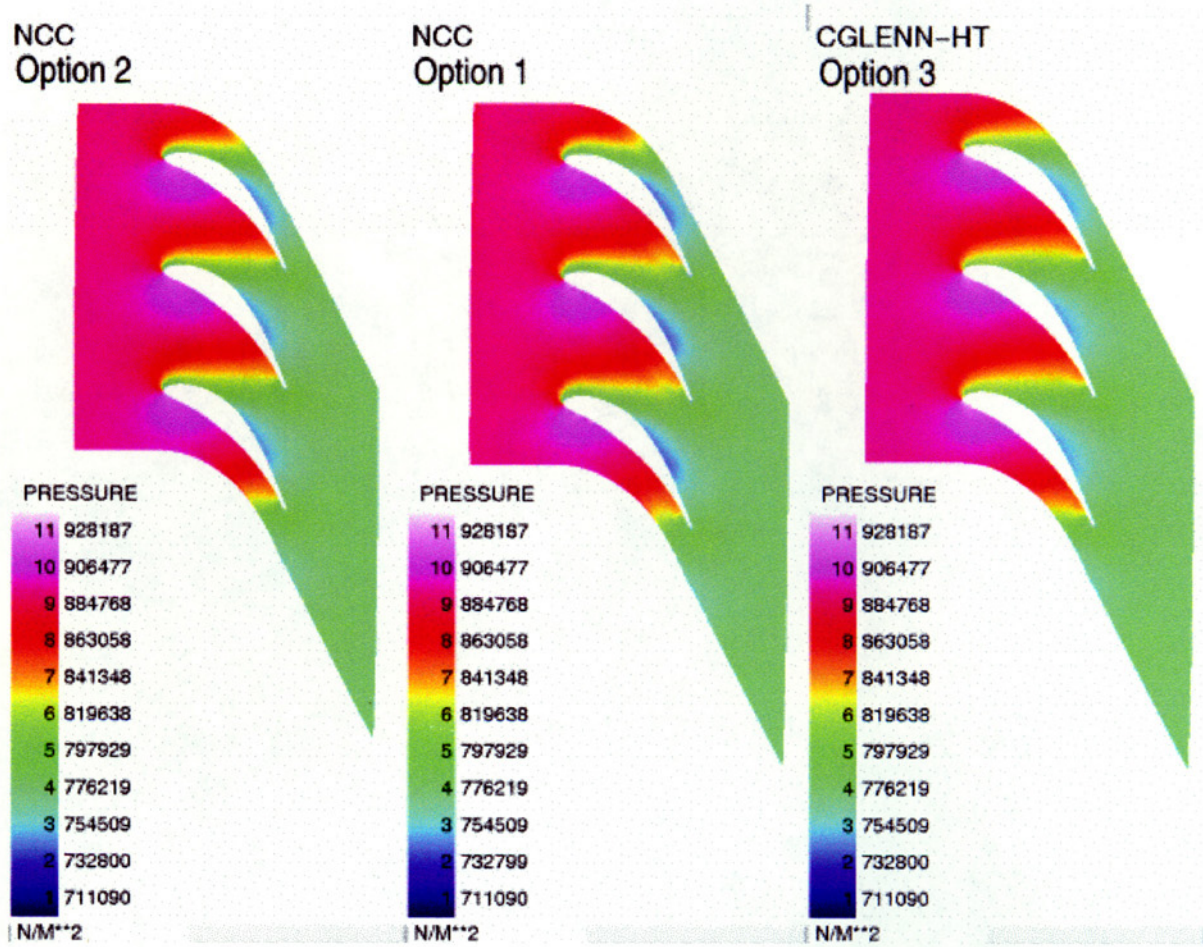
Figure 9: Comparison of the pressure distribution.
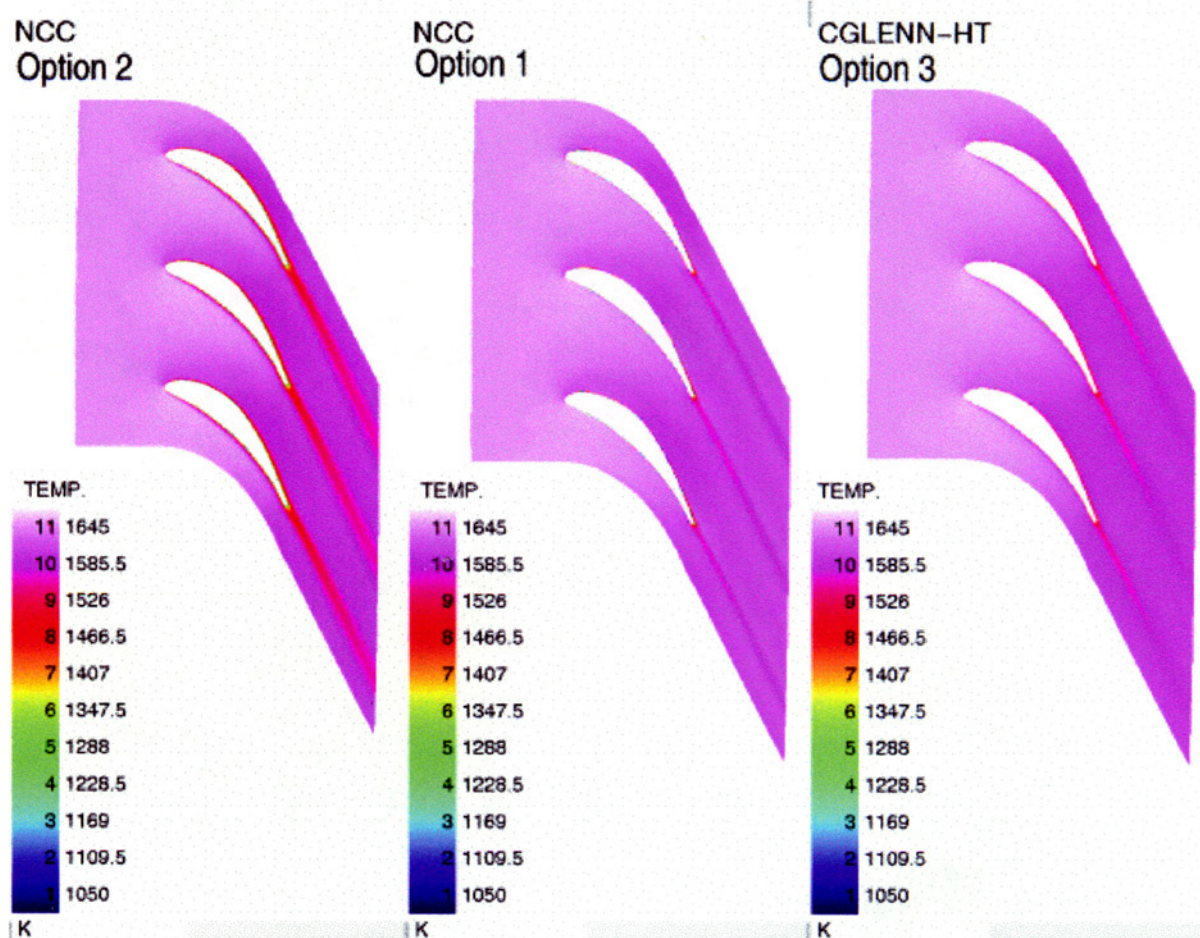
Figure 10: Comparison of the temperature distribution.
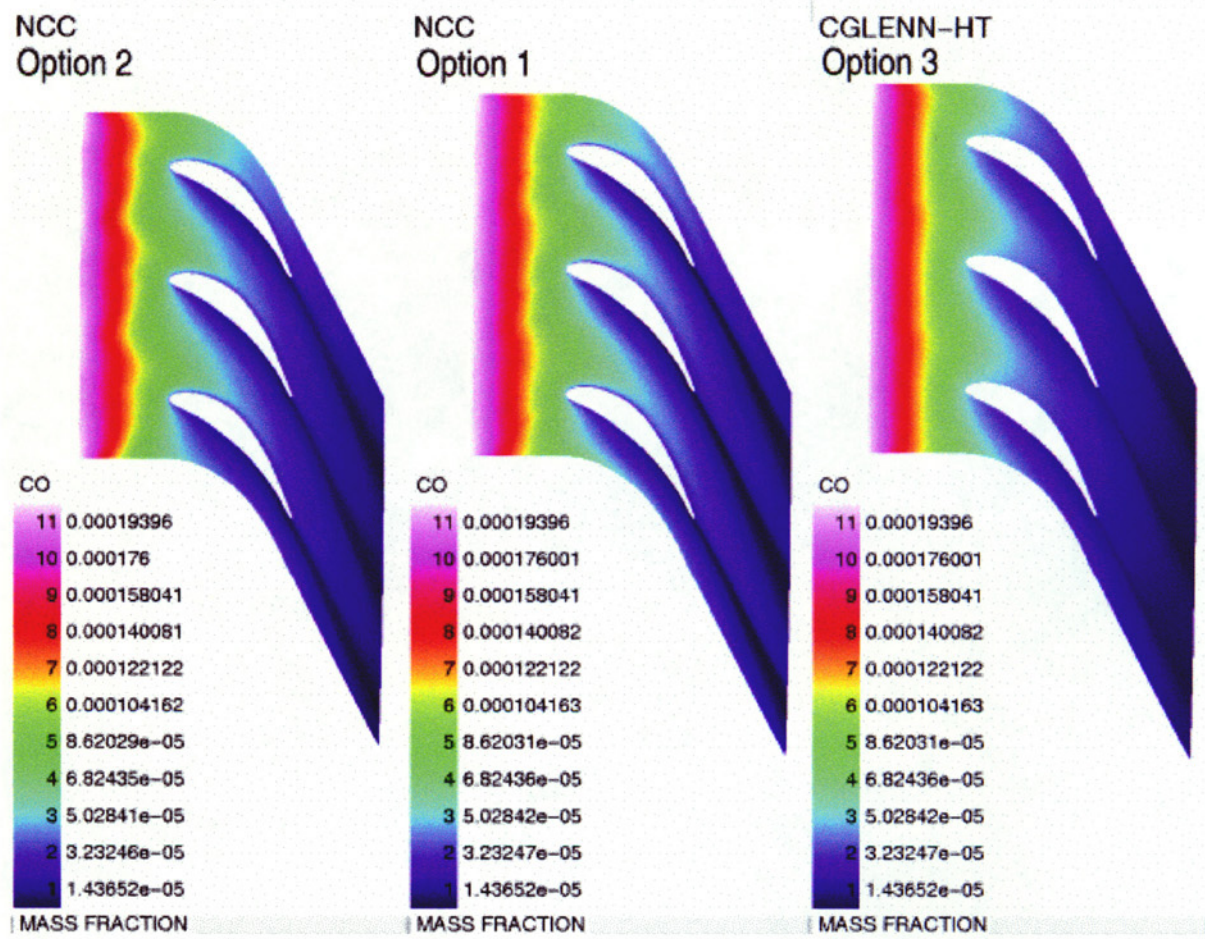
Figure 11: Comparison of the CO distribution.

NCC
Option 2

NCC
Option 1

CGLENN-HT
Option 3

NO	
11	0.000132433
10	0.000130192
9	0.000127951
8	0.00012571
7	0.000123469
6	0.000121227
5	0.000118986
4	0.000116745
3	0.000114504
2	0.000112263
1	0.000110022

MASS FRACTION

NO	
11	0.000132433
10	0.000130192
9	0.000127951
8	0.00012571
7	0.000123468
6	0.000121227
5	0.000118986
4	0.000116745
3	0.000114504
2	0.000112263
1	0.000110022

MASS FRACTION

NO	
11	0.000132433
10	0.000130192
9	0.000127951
8	0.00012571
7	0.000123468
6	0.000121227
5	0.000118986
4	0.000116745
3	0.000114504
2	0.000112263
1	0.000110022

MASS FRACTION

Figure 12: Comparison of the N O distribution.
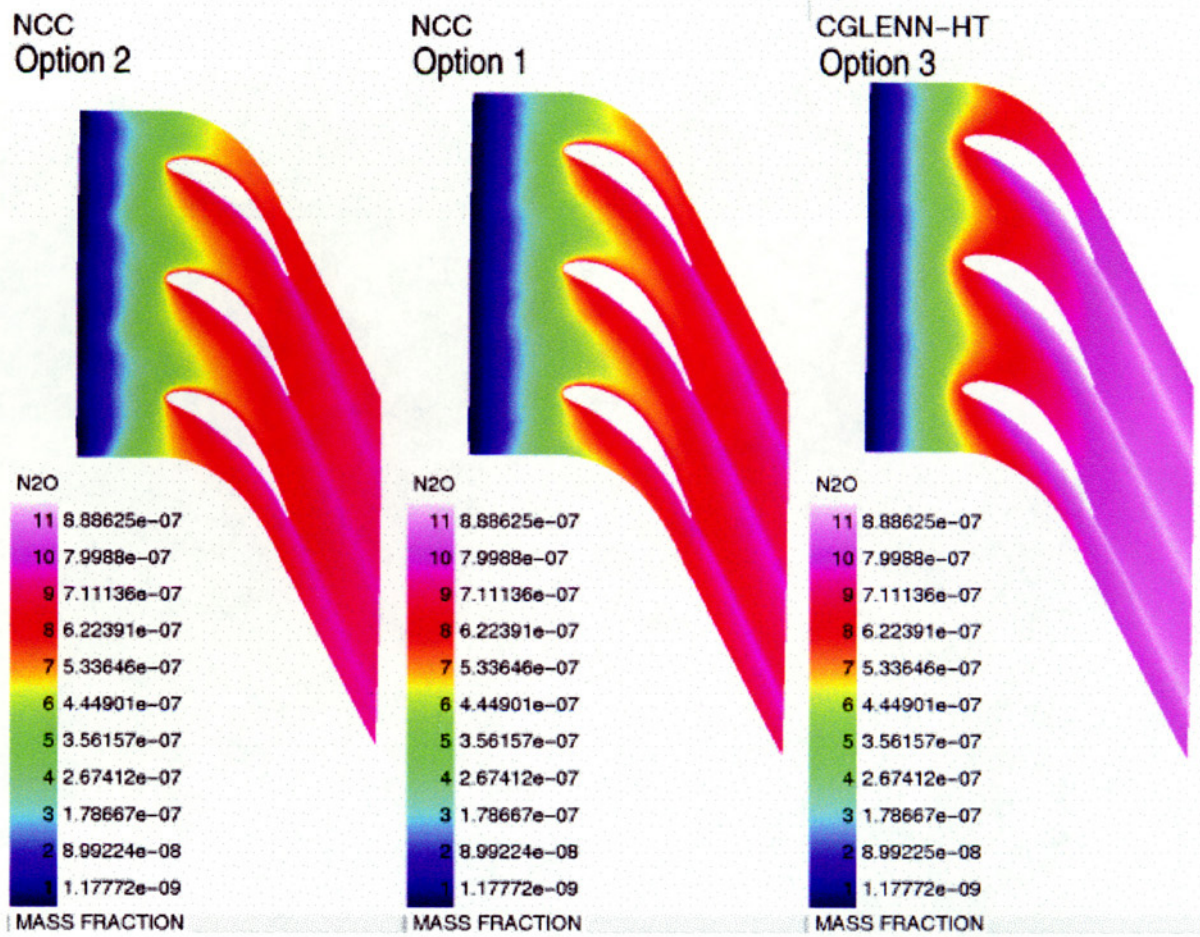
Figure 13: Comparison of the N_2O distribution.
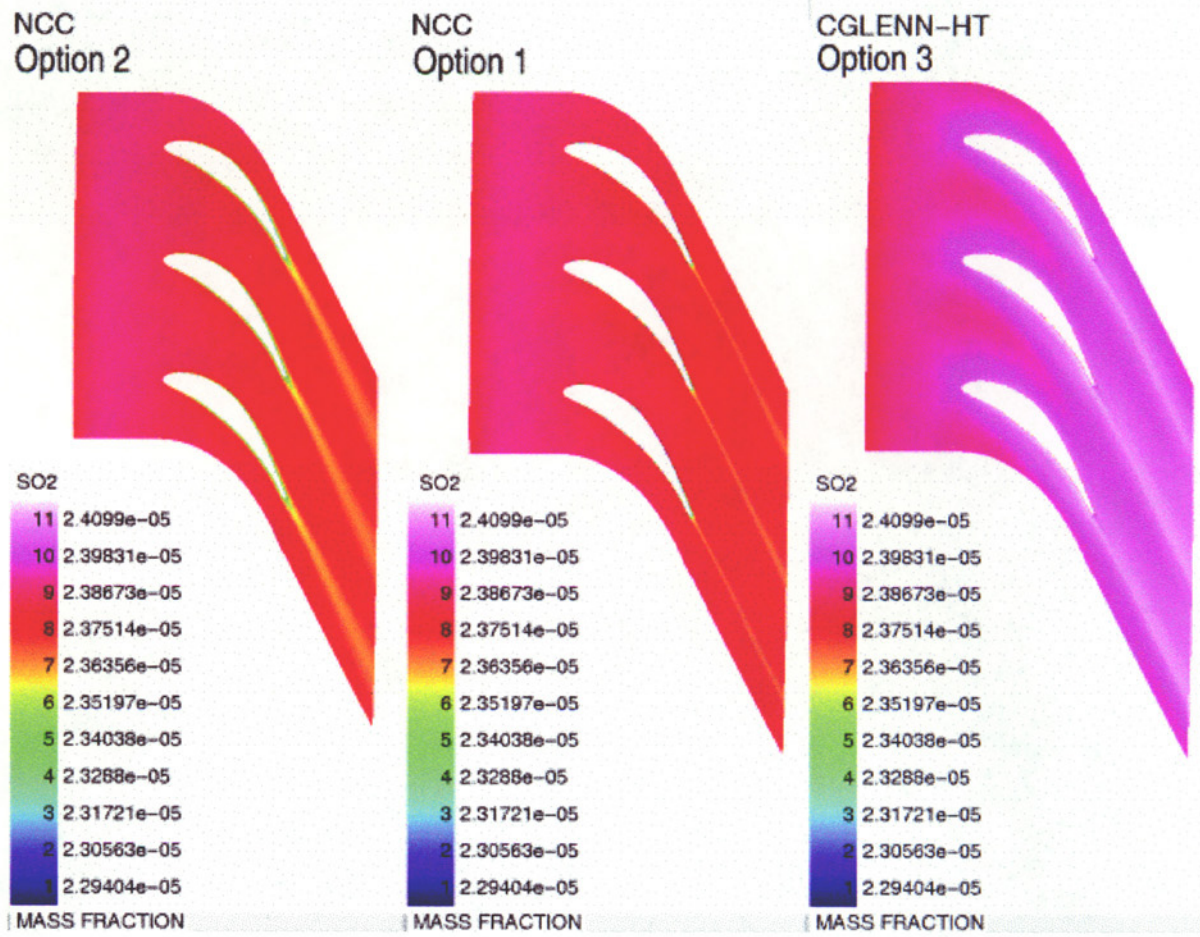
Figure 14: Comparison of the SO_2 distribution.
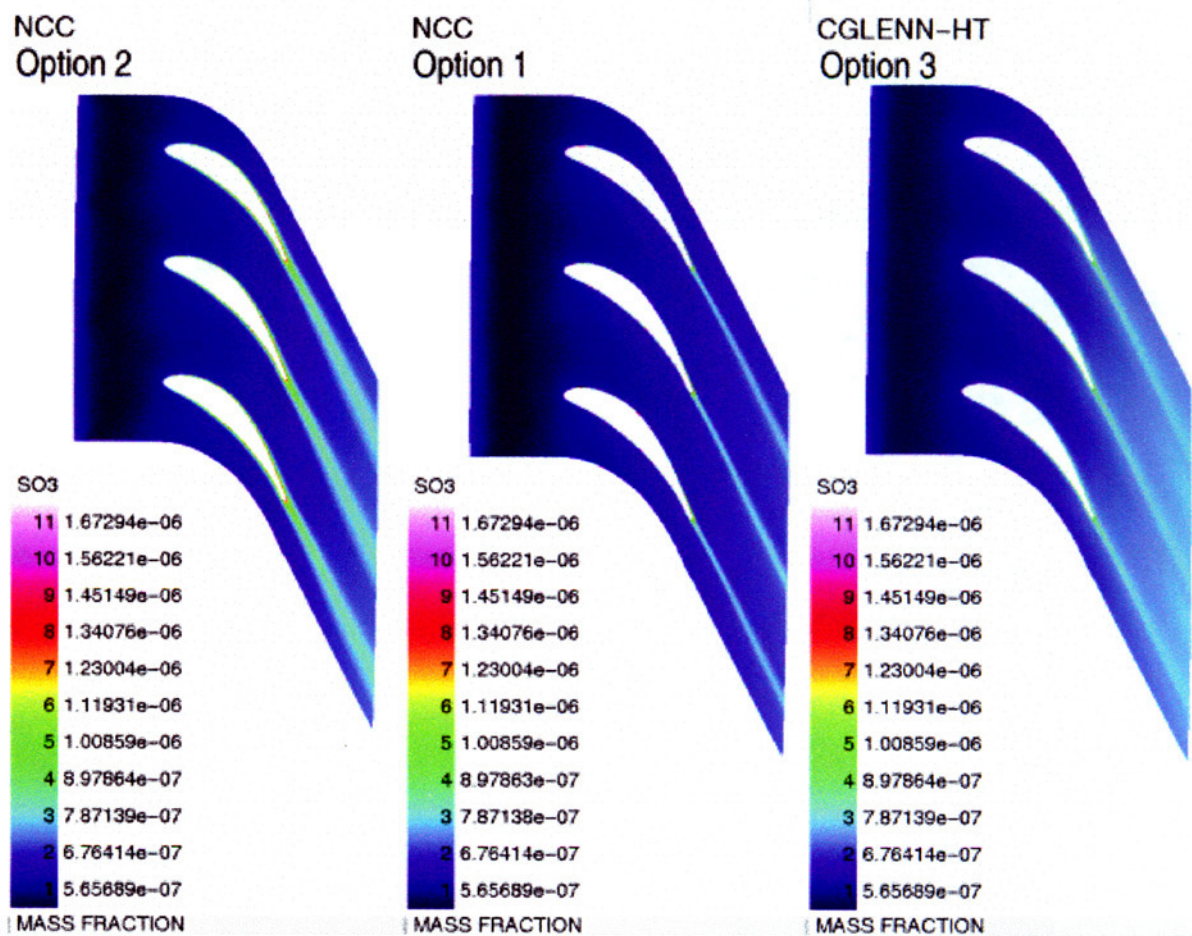
Figure 15: Comparison of the SO_3 distribution.

As an attemp to reconcile these differences, the Roe's upwind algorithm is used both in the NCC and the CGLENN-HT to conduct the calculations. This will minimize the differences due to the treatment of the convective terms. Furthermore, the terms representing the species mass diffusion in the species equations are dropped off from CGLENN-HT. From Figure 16 to Figure 19, it can be seen that the differences of the solution of NO and SO_2 are now less appreciable than those previously indicated in Figure 12 and Figure 14.
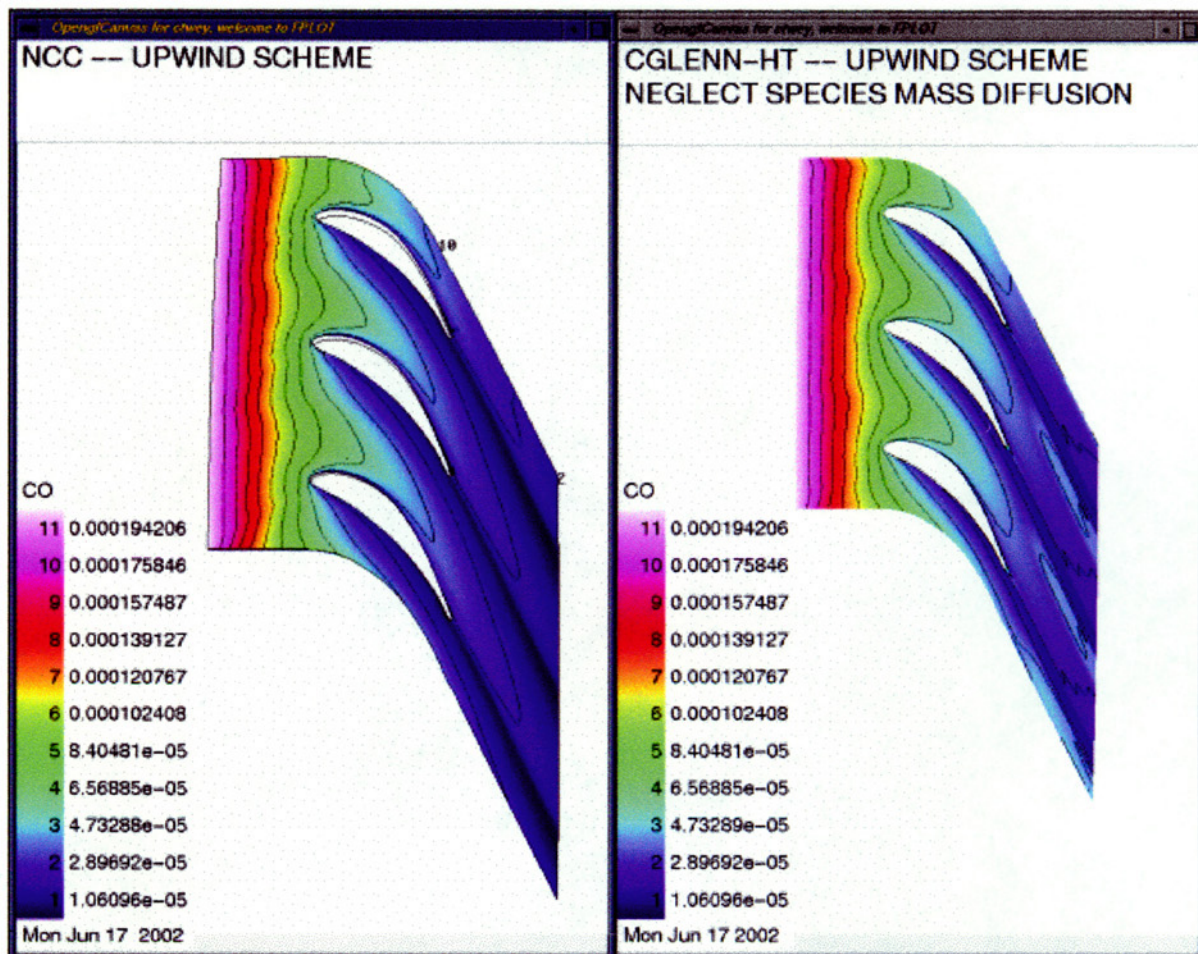

Figure 16: Comparison of the CO distribution.
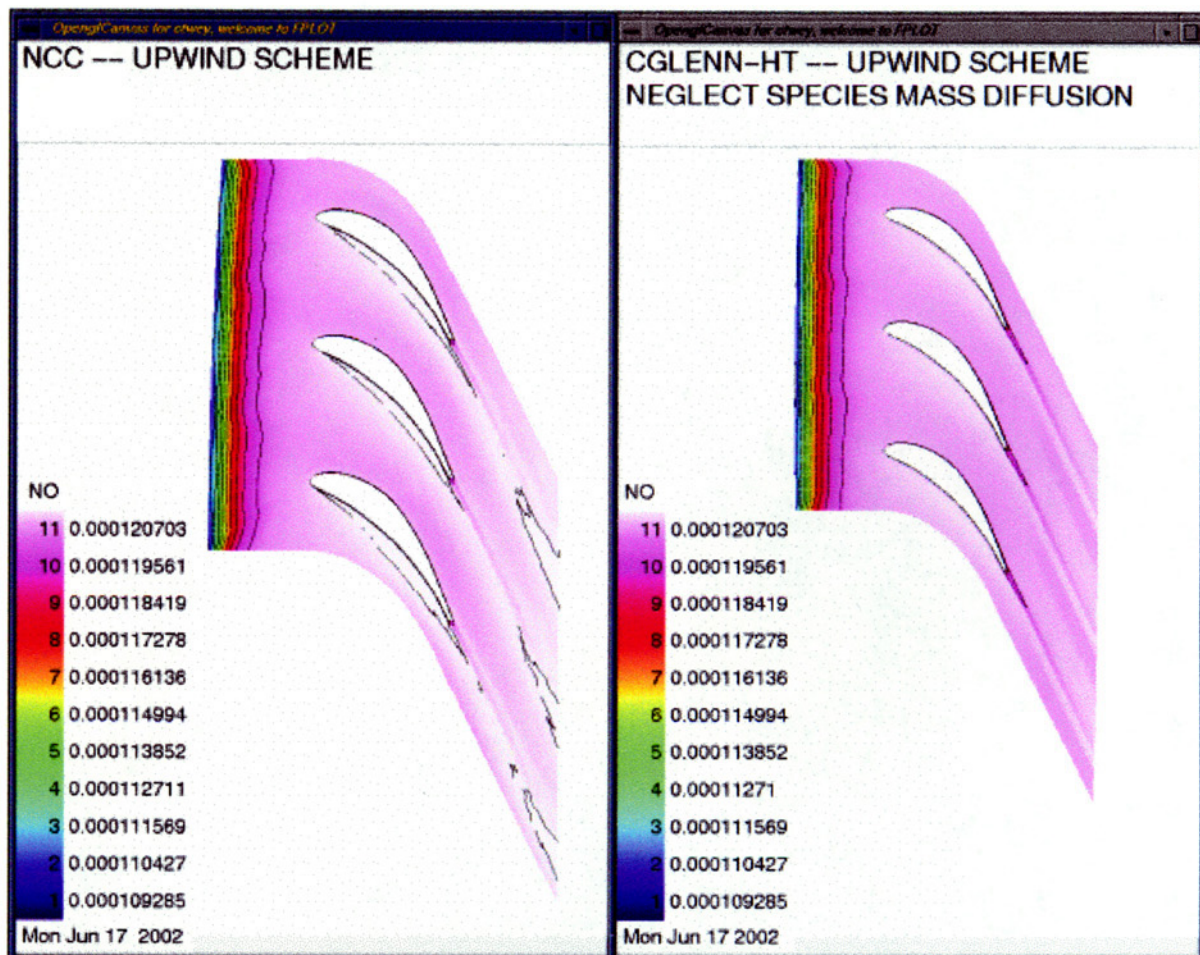
Figure 17: Comparison of the NO distribution.
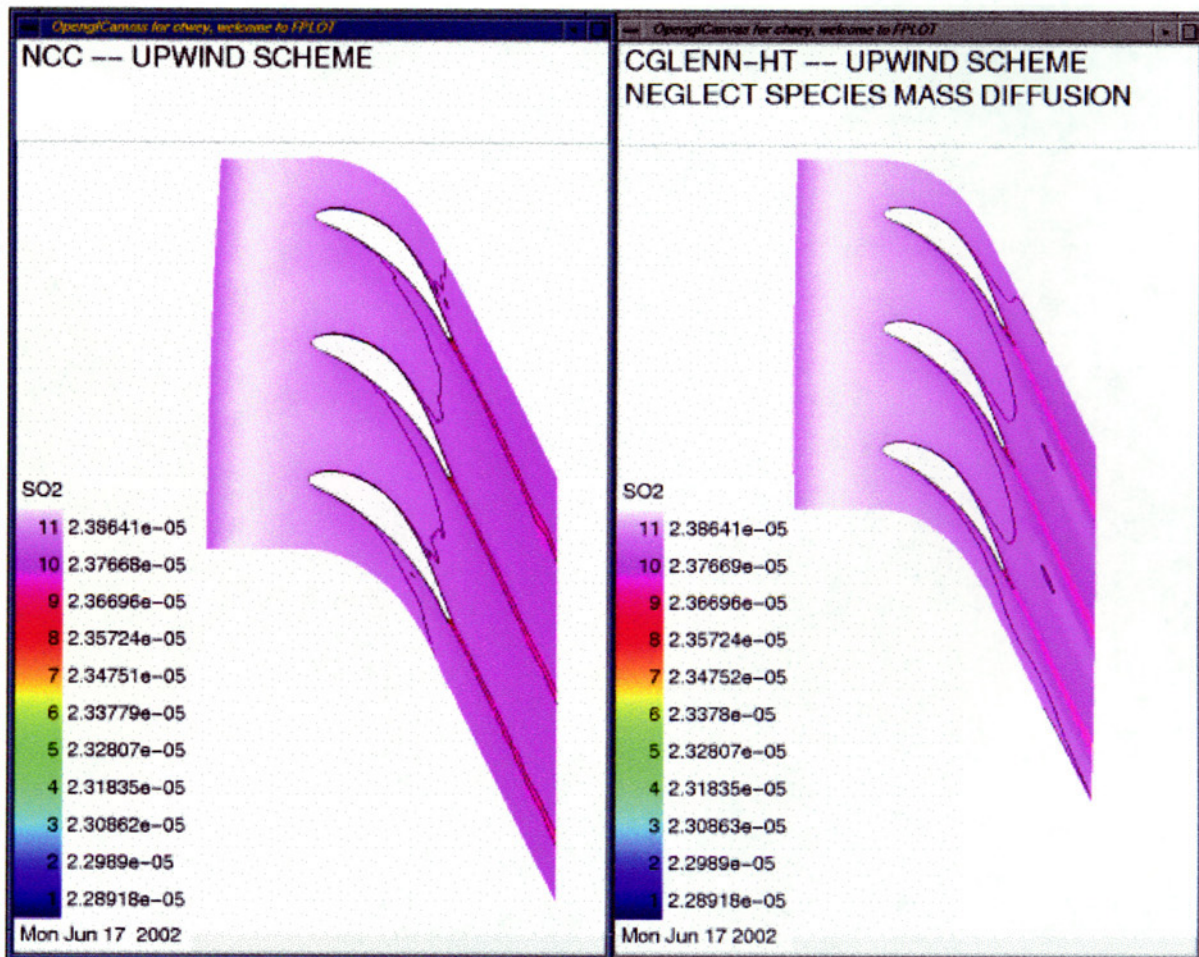
Figure 18: Comparison of the SO_2 distribution.
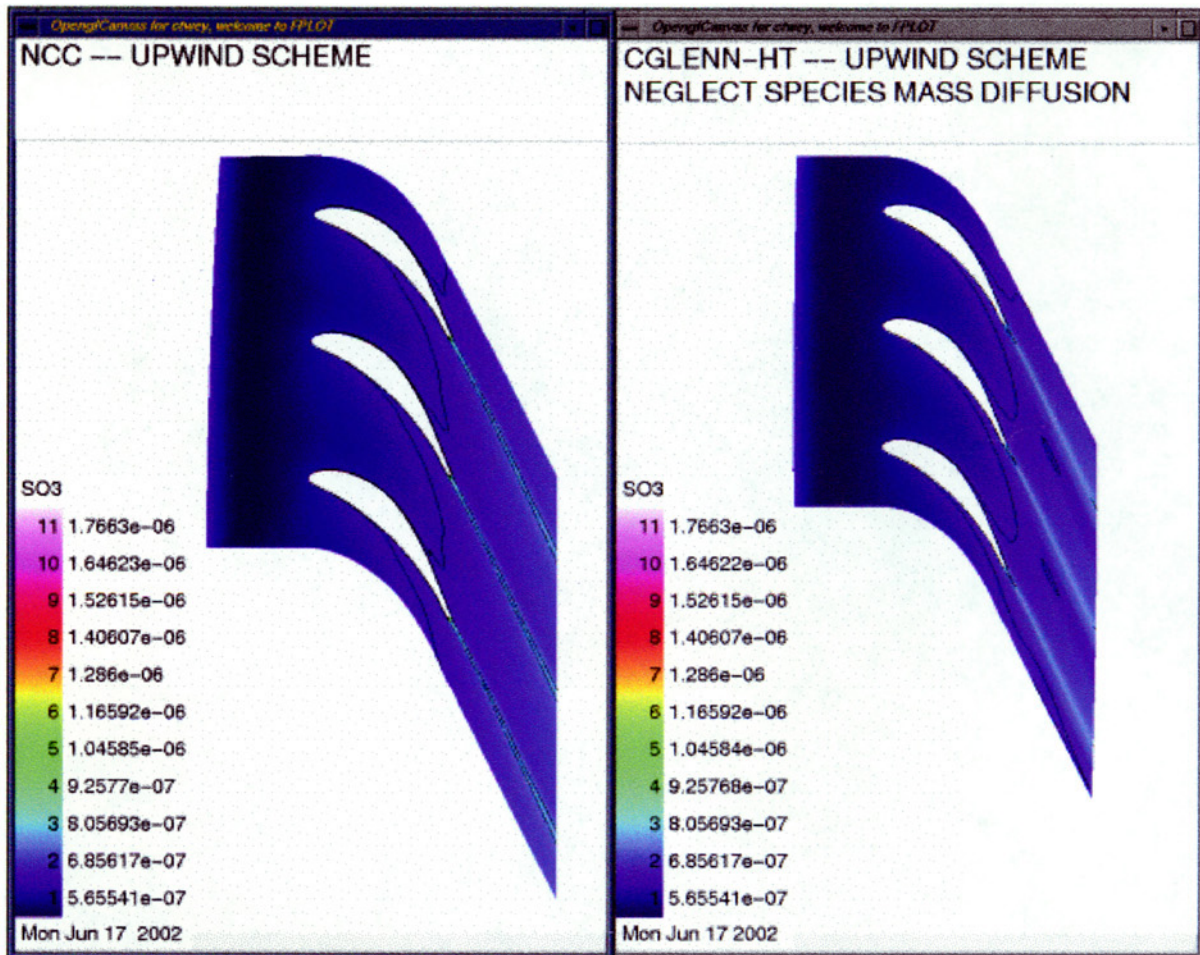
Figure 19: Comparison of the SO_3 distribution.

8.3.2 Absolute Inlet Boundary Conditions

The total temperature is 1631.7 K and the swirl angle is 64°, viewed from a stationary reference frame. Five sets of computed results are assembled together to show the differences due to various codes and options. They are (1) CGLENN-HT using option 3 with structured hexahedron, (2) NCC using option 1 with unstructured hexahedron, (3) NCC using option 2 with unstructured hexahedron, (4) CNEWT/GRC using option 2 with unstructured hexahedron, (5) CNEWT/MIT using option 2 with tetrahedron. Data reduction technique has been used to average the CFD results to get 1D distribution along the axis of the flow path.

The area-averaged pressure distributions along the axis of the flow path are shown in Figure 20. It indicates that the differences among the five cases are minimal for the pressure except in the front part of the domain.
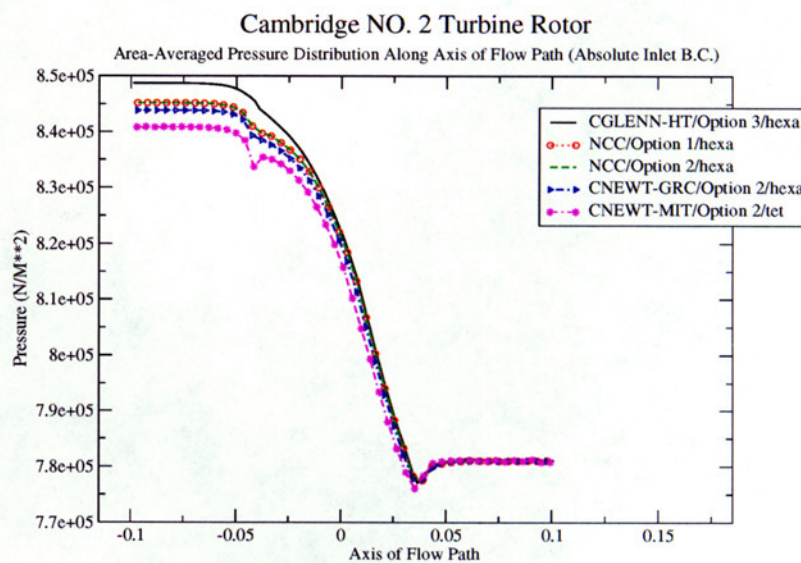

Figure 20: Comparison of pressure distribution along the axis of the flow path.

The temperature distributions along the axis of the flow path are shown in Figure 21.


Cambridge NO. 2 Turbine Rotor
Area-Averaged Temperature Distribution Along Axis of Flow Path (Absolute Inlet B.C.)
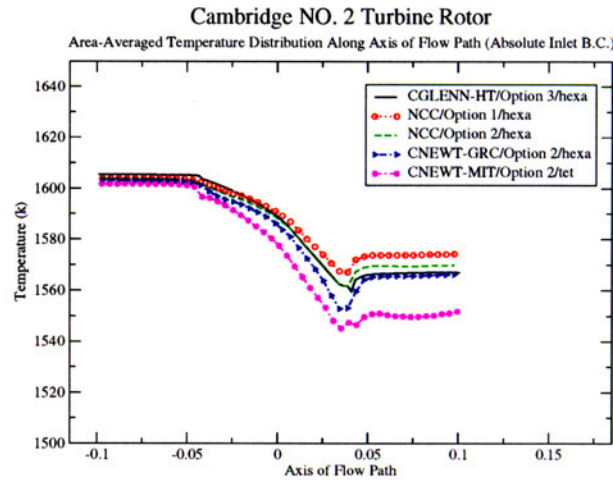
Figure 21: Comparison of the temperature distribution along the axis of the flow path.

CO distributions are shown in Figure 22. The mass fraction decreases as the flow passing through the turbine passage.


Cambridge NO. 2 Turbine Rotor
Area-Averaged CO Distribution Along Axis of Flow Path (Absolute Inlet B.C.)
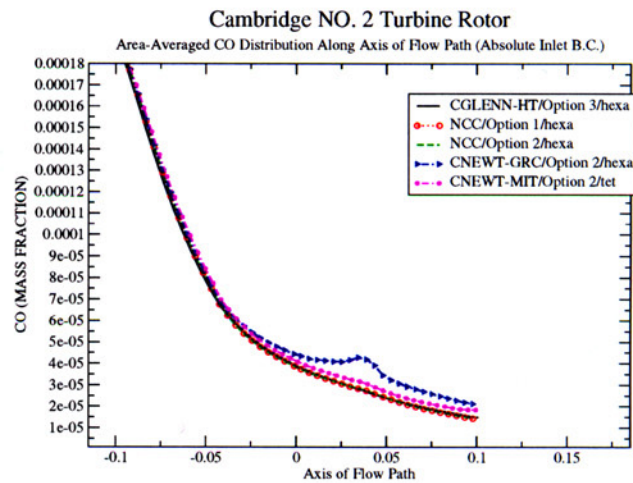
Figure 22: Comparison of the CO distribution along the axis of the flow path.

NO distributions are shown in Figure 23. The mass fraction increases significantly at first then remains nearly constant as the flow passing through the turbine passage.
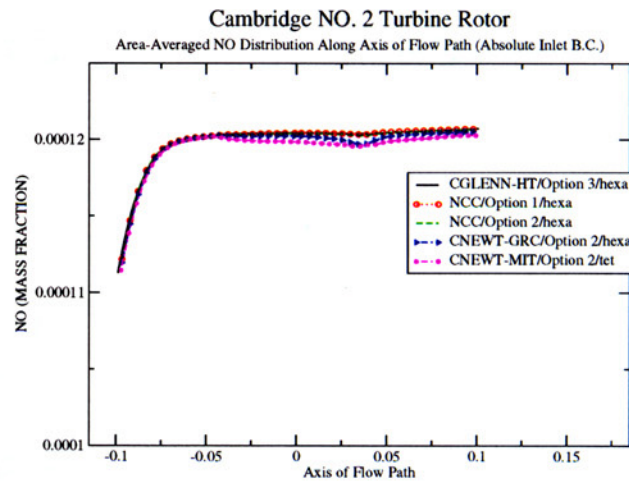

Figure 23: Comparison of NO distribution along the axis of the flow path.

NO_2 distributions are shown in Figure 24.
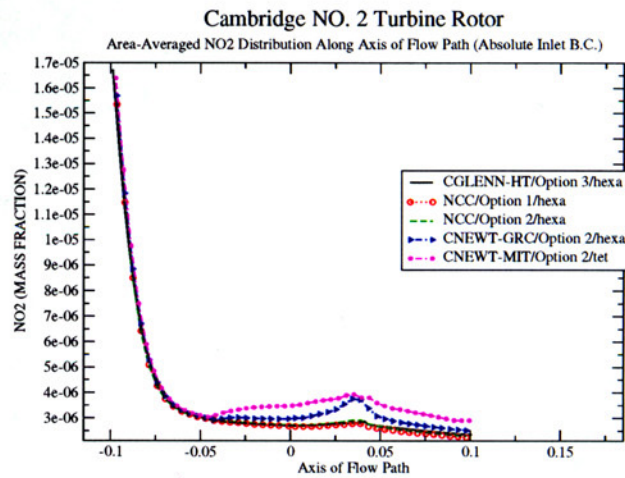
Figure 24: Comparison of the NO_2 distribution along the axis of the flow path.

SO_2 distributions are shown in Figure 25.
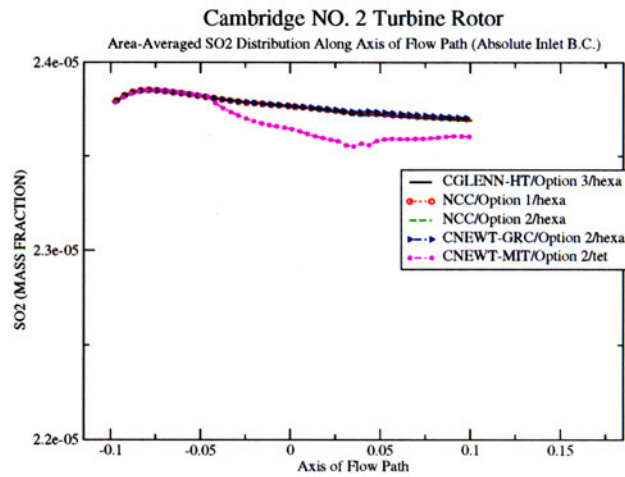
Figure 25: Comparison of the SO_2 distribution along the axis of the flow path.

SO_3 distributions are shown in Figure 26. The solution of CNEWT/MIT deviates signifcantly from that of other computations.
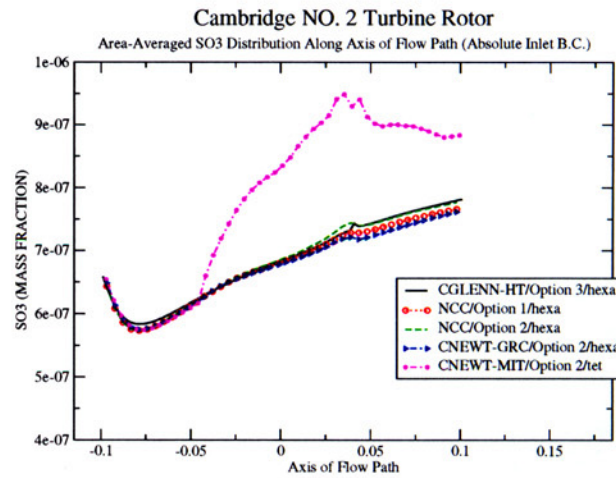
Figure 26: Comparison of the SO_3 distribution along the axis of the flow path.

HONO distributions are shown in Figure 27. The mass fraction obtained from CNEWT/MIT using tetrahedron shows more activity than that obtained from other computations.
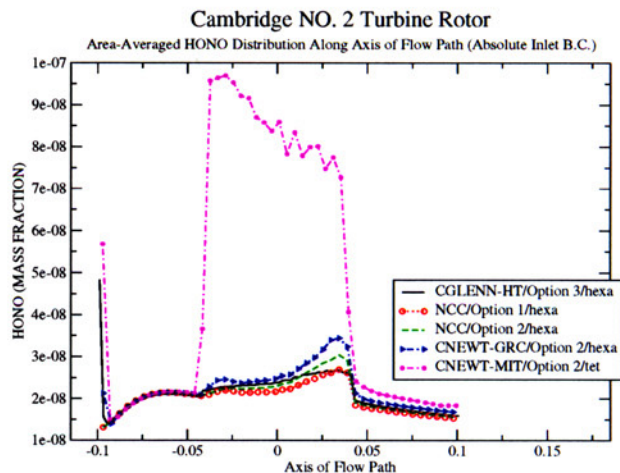

Figure 27: Comparison of the *HONO* distribution along the axis of the flow path.

Velocity distributions are shown in Figure 28.
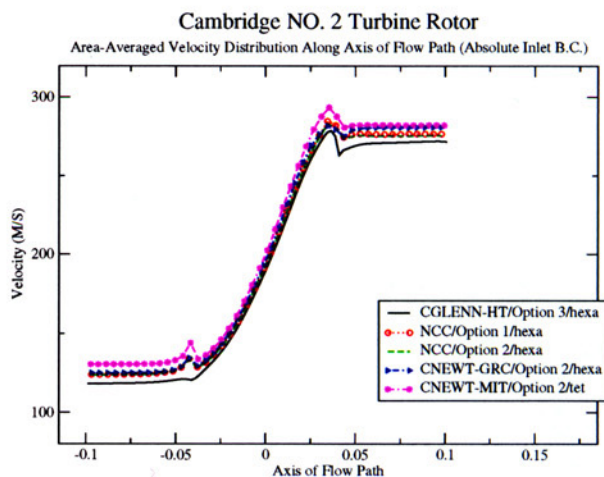
Figure 28: Comparison of velocity distribution along the axis of the flow path.

8.4   The Impact of the Mesh Shape

At this point, a note on the impact of the mesh shape on the computing time is in order. A tetrahedral mesh used by CNEWT for the case of Cambridge's NO.2 rotor was converted to NCC format via FPLOT, and NCC computations were performed using this tetrahedral mesh. A tetrahedral mesh will usually increase the overall element count, and for a cell-center based algorithm, this in turn will increase the frequency of chemical source term evaluation. This kind of impact becomes significant when the number of species becomes sufficiently large, such as the case of trace chemistry mechanism. The CPU time statistics for NCC using hexahedral and tetrahedral meshes are summarized in Table 1

NCC	Hexahedron	Tetrahedron
grid points	100980	37135
elements	79056	171636
facets	280594	224845
boundary facets	43000	32144
CPU time (sec/iteration step)	538	1125

Table 1: Run time statistics for NCC using hexahedral and tetrahedraon meshes.

When using the tetrahedral mesh, NCC not only consumes more CPU time per iteration step but also needs many more number of iterations to reach the convergence. The main reason for longer CPU time per step using tetrahedral mesh is that NCC needs to compute the species production rate 171636 times per step, while only 79056 times are required for the hexahedral mesh. The main resaon for more iteration numbers needed for convergence is that the number of information exchange among tetrahedral elements is four, while that number is six for a hexahedral element. Thus, less amount of information is exchanged per step among the tetrahedral elements.

9   Concluding Remarks

The goal of the present effort is to establish GRC/NASA in-house capability for modeling and simulation of intra-engine trace chemical changes over post-combustor flow path. The coding effort to port the trace chemistry model in CNEWT to GLENN-HT and NCC has completed. In addition to the implementation of trace chemistry model to existing CFD codes, several pre/post-processing tools that can handle the manipulations of the geometry, the unstructured and multi-block structured grids, as well as CFD solutions have been enhanced and seamlessly tied with NCC, CGLENN-HT and CNEWT/GRC. These tools have been applied to several test cases.

The existing tool kit consists of the following software:

1. cfe_NASA — A MATLIB script to generate species mass fractions at a combustor exit using CHEMKIN III libraray which is a commercial extension of CHEMKIN II.

2. CKINTERP — A program to create a CHEMKIN II linking file for reaction rate parameters and chemical mechanism. It takes the output of cfe_NASA and generates a file called *chem.bin* for use in CALCHEM, CNEWT/GRC, CGLENN-HT and NCC.

3. CALCHEM — A program for one-dimensional intra-engine trace chemistry analysis.

4. T3D, FPLOT, OVERGC — pre/post-processing codes.

5. CNEWT/GRC, CGLENN-HT, NCC — chemistry flow solvers.

Thus a complete CFD package consisting of pre/post-processing tools and flow solvers suitable for the post-combustor intra-engine trace chemistry study has been assembled.

References

[1] S. P. Lukachko, I. A. Waitz, R. C. Miake-Lye, R. C. Brown and M. R. Anderson, "Production of Sulfate Aerosol Precursors in The Turbine and Exhaust Nozzle of An Aircraft Engine," Journal of Geophysical Research Vol.103, NO.D13, Pages 16.159-16.174, July 20, 1998.

[2] A. T. Chobot, "Modeling The Evolution of Trace Species in The Post-Combustor Flow Path Of Gas Turbine Engines," S.M. Thesis. Massachusetts Institute of Technology, Sept., 2000.

[3] E. Steinthorsson, A. A. Ameri and David L. Rigby, "LeRC-HT, The NASA Lewis Research Center General Multi-Block Navier-Stokes Convective Heat Transfer Code," GRC/NASA, Ohio, January 15, 1999.

[4] R. M. Stubbs and N. S. Liu, "Preview of National Combustion Code," AIAA 97-3114, 1997.

[5] Thomas Wey and Nan-Suey Liu, "Film Cooling Flow Effects On Post-Combustor Trace Chemistry", Sept. 2002, submitted for publication as a NASA TM.

[6] T. C. Wey, "The Applications Of An Unstructured Grid Based Overset Grid Scheme To Applied Aerodynamics," 8th International Meshing Roundtable, Oct., 1999.

[7] T. C. Wey, "Unstructured Hexahedral Mesh Generation Using the Analogy of the Particle Traces — Dual Use of Overset Grid Generation Techniques," AIAA 2001-1097, 39th Aerospace Sciences Meeting and Exhibit January 8–11, 2001/Reno, NV

[8] T. C. Wey, "Development of A Mesh Interface Generator For Overlapped Structured Grids", AIAA 94-1924, AIAA 12th Applied Aerodynamics Conference, June 20-22, 1994/Colorado Spring, CO.

REPORT DOCUMENTATION PAGE

Public reporting burden for this collection of information is estimated to average 1 hour per response, including the time for reviewing instructions, searching existing data sources, gathering and maintaining the data needed, and completing and reviewing the collection of information. Send comments regarding this burden estimate or any other aspect of this collection of information, including suggestions for reducing this burden, to Washington Headquarters Services, Directorate for Information Operations and Reports, 1215 Jefferson Davis Highway, Suite 1204, Arlington, VA 22202-4302, and to the Office of Management and Budget, Paperwork Reduction Project (0704-0188), Washington, DC 20503.

1. AGENCY USE ONLY (Leave blank)	2. REPORT DATE March 2003	3. REPORT TYPE AND DATES COVERED Technical Memorandum

4. TITLE AND SUBTITLE

Current Status of Post-Combustor Trace Chemistry Modeling and Simulation at NASA Glenn Research Center

6. AUTHOR(S)

Thomas Wey and Nan-Suey Liu

5. FUNDING NUMBERS

WBS–22–714–01–03

7. PERFORMING ORGANIZATION NAME(S) AND ADDRESS(ES)

National Aeronautics and Space Administration
John H. Glenn Research Center at Lewis Field
Cleveland, Ohio 44135–3191

8. PERFORMING ORGANIZATION REPORT NUMBER

E–13785

9. SPONSORING/MONITORING AGENCY NAME(S) AND ADDRESS(ES)

National Aeronautics and Space Administration
Washington, DC 20546–0001

10. SPONSORING/MONITORING AGENCY REPORT NUMBER

NASA TM—2003-212184

11. SUPPLEMENTARY NOTES

Thomas Wey, Taitech, Inc., Beavercreek, Ohio 45430; and Nan-Suey Liu, NASA Glenn Research Center. Responsible person, Thomas Wey, organization code 5830, 216–433–2934.

12a. DISTRIBUTION/AVAILABILITY STATEMENT

Unclassified - Unlimited
Subject Category: 07   Distribution: Nonstandard

Available electronically at http://gltrs.grc.nasa.gov

This publication is available from the NASA Center for AeroSpace Information, 301–621–0390.

12b. DISTRIBUTION CODE

13. ABSTRACT (Maximum 200 words)

The overall objective of the current effort at NASA GRC is to evaluate, develop, and apply methodologies suitable for modeling intra-engine trace chemical changes over post combustor flow path relevant to the pollutant emissions from aircraft engines. At the present time, the focus is the high pressure turbine environment. At first, the trace chemistry model of CNEWT were implemented into GLENN-HT as well as NCC. Then, CNEWT, CGLENN-HT, and NCC were applied to the trace species evolution in a cascade of Cambridge University's No. 2 rotor and in a turbine vane passage. In general, the results from these different codes provide similar features. However, the details of some of the quantities of interest can be sensitive to the differences of these codes. This report summaries the implementation effort and presents the comparison of the No. 2 rotor results obtained from these different codes. The comparison of the turbine vane passage results is reported elsewhere. In addition to the implementation of trace chemistry model into existing CFD codes, several pre/post-processing tools that can handle the manipulations of the geometry, the unstructured and structured grids as well as the CFD solutions also have been enhanced and seamlessly tied with NCC, CGLENN-HT, and CNEWT. Thus, a complete CFD package consisting of pre/post-processing tools and flow solvers suitable for post-combustor intra-engine trace chemistry study is assembled.

14. SUBJECT TERMS

Emissions

15. NUMBER OF PAGES
43

16. PRICE CODE

17. SECURITY CLASSIFICATION OF REPORT Unclassified	18. SECURITY CLASSIFICATION OF THIS PAGE Unclassified	19. SECURITY CLASSIFICATION OF ABSTRACT Unclassified	20. LIMITATION OF ABSTRACT

NSN 7540-01-280-5500

Standard Form 298 (Rev. 2-89)
Prescribed by ANSI Std. Z39-18
298-102